

ScholarWorks@GSU

Functional Analysis of the Murine Oligoadenylate Synthetase 1b (Oas1b)

Authors	Elbahesh, Husni
Citation	Elbahesh, Husni. (2006). Functional Analysis of the Murine Oligoadenylate Synthetase 1b (Oas1b). Georgia State University. https://doi.org/10.57709/1059198
DOI	https://doi.org/10.57709/1059198
Rights	<p>I hereby certify that, if appropriate, I have obtained and attached hereto a written permission statement from the owner(s) of each third party copyrighted matter to be included in my thesis, dissertation, or project report, allowing distribution as specified below. I certify that the version I submitted is the same as that approved by my advisory committee. I hereby grant to Georgia State University or its agents the non-exclusive license to archive and make accessible, under the conditions specified below, my thesis, dissertation, or project report in whole or in part in all forms of media, now or hereafter known. I retain all other ownership rights to the copyright of the thesis, dissertation or project report. I also retain the right to use in future works (such as articles or books) all or part of this thesis, dissertation, or project report.</p>
Download date	2026-04-10 22:45:26
Link to Item	https://hdl.handle.net/20.500.14694/2276

FUNCTIONAL ANALYSIS OF THE MURINE OLIGOADENYLATE

SYNTHETASE 1b (Oas1b)

by

HUSNI ELBAHESH

Under the direction of Margo A. Brinton

ABSTRACT

The flavivirus resistance gene, *Flv*, in mice has been identified as 2'-5' oligoadenylate synthetase 1b (Oas1b). Susceptible mice produce a protein that is truncated (Oas1btr) at the C-terminus due to a premature stop codon encoded by a C820T transition. Mice produce 8 Oas1 proteins, Oas1a-Oas1h. In the present study, Oas1a, Oas1b and Oas1btr were expressed as MBP-fusion proteins in bacteria and purified. 2-5A synthetase activity was demonstrated using MBP-Oas1a, while neither MBP-Oas1b nor MBP-Oas1btr were functionally active. The 2-5A synthetase activity of MBP-Oas1a was inhibited in a dose-dependent manner by the addition of MBP-Oas1b but not MBP-Oas1btr. Finally, three RNA probes were synthesized from the 3' end of the WNV Eg101 genome and used to test the ability of the expressed Oas1 proteins to bind to viral RNA. Results of the RNA binding activity assays suggest Oas1 proteins may specifically interact with regions of WNV RNA.

INDEX WORDS: Oligoadenylate synthetase, Flavivirus, West Nile virus, Viral RNA

**FUNCTIONAL ANALYSIS OF THE MURINE OLIGOADENYLATE
SYNTHETASE 1b (Oas1b)**

by

HUSNI ELBAHESH

A Thesis Submitted in Partial Fulfillment of Requirements for the Degree of
Master in Science
in the College of Arts and Sciences
Georgia State University

2005

Copyright by
Husni Muhammad Hisham Elbahesh
2005

**FUNCTIONAL ANALYSIS OF THE MURINE OLIGOADENYLATE
SYNTHETASE 1b (Oas1b)**

by

HUSNI ELBAHESH

Major Professor: Margo A. Brinton

Committee: Teryl K. Frey

Zehava Eichenbaum

Electronic Version Approved:

Office of Graduate Studies
College of Arts and Sciences
Georgia State University
December 2005

ACKNOWLEDGMENT

I would like to extend my sincerest appreciation to my principal advisor Dr. Margo A. Brinton who allowed me to work in her lab and complete this project. I would like to thank Dr. Brinton for her support, patience, and expert advice. Thanks to the committee members Dr. Teryl Frey and Dr. Zehava Eichenbaum for their suggestions and corrections. I would especially like to thank Dr. Svetlana V. Scherbik for her technical advice, tremendous patience, and her help. Without her guidance, completion of this project would not have been possible. Thanks to William G. Davis and Mohamed M. Emara for their help and advice on many of the experiments performed during this project.

TABLE OF CONTENTS

ACKNOWLEDGMENTS	iv
TABLE OF CONTENTS	v
LIST OF FIGURES	vi
LIST OF ABBREVIATIONS	vii
INTRODUCTION	1
MATERIALS AND METHODS	18
RESULTS	26
DISCUSSION	56
BIBLIOGRAPHY	64

LIST OF FIGURES

Figure	Page
1. Expression of Oas1a, Oas1b and Oas1btr proteins in bacteria.	27
2. Purification of Oas1 proteins.	29
3. Representative western of MBP-Oas1 proteins purified by amylose resin.	30
4. Cleavage of Oas1a from MBP by Genenase I.	31
5. Analysis of cleavage products by western blotting.	33
6. Analysis of the 2-5A synthetase activity of MBP-Oas1a.	36
7. Analysis of the 2'-5' OAS activity of MBP-Oas1b protein.	38
8. Secondary structure predictions of the three WNV RNA probes.	40
9. Gel mobility shift assay to determine the optimal non-specific competitor concentration.	42
10. Gel mobility shift assay with (+) 3' UA Probe #1.	43
11. Effect of MBP-Oas1b concentration on binding activity to (+) 3' UA Probe #1.	45
12. Effect of MBP-Oas1a concentration on binding activity to (+) 3' UA Probe #1.	46
13. Effect of MBP-Oas1btr concentration on binding activity to (+) 3' UA Probe#1.	47
14. Gel mobility shift assay with (+) 3' Control Probe #2.	49
15. Gel mobility shift assay with (+) 3' Control Probe #2.	50
16. Gel mobility shift assay with (+) 3' SL Probe #3.	52
17. Gel mobility shift assay with (+) 3' SL Probe #3.	53
18. Inhibition of MBP-Oas1a synthetase activity.	55

LIST OF ABBREVIATIONS

- AMP:** Ampicillin
- ATP:** Adenosine triphosphate
- β-ME:** β-Mercaptoethanol
- bp:** Base pair
- BSA:** Bovine serum albumin
- cDNA:** Complementary DNA
- cM:** CentiMorgans
- CRB:** Carbenicillin
- C-terminus:** Carboxyl terminus
- DNA:** Deoxyribonucleic acid
- DRAF:** DsRNA activated factor
- ds:** Double-stranded
- dsRBM:** DsRNA binding motif
- DTT:** Dithiothreitol
- DV:** Dengue virus
- EF1A:** Translation elongation factor 1A
- ER:** Endoplasmic reticulum
- Flv:** Flavivirus resistance gene
- HRP:** Horseradish peroxidase
- IFN:** Interferon
- IPTG:** Isopropyl-β-d-thiogalactopyranoside

IRF: IFN regulatory factor

ISG: IFN stimulated genes

ISGF: IFN stimulated gene factor

ISRE: IFN-stimulated response element

JAK: Janus protein tyrosine kinase

JEV: Japanese encephalitis virus

kDa: Kilo Dalton

LB: Luria-Bertani media

LI: Louping ill

MBP: Maltose binding protein

mRNA: Messenger RNA

MVEV: Murray Valley fever virus

N-terminus: Amino terminus

NTPase: Nucleotidyl phosphatase

OAS: 2'-5' oligoadenylate synthetase

ORF: Open reading frame

PCR: Polymerase chain reaction

PFU: Plaque forming unit

PKR: Protein kinase RNA regulated protein

Poly(I:C): Polyinosinic:polycytidylic acid

PRD: Positive regulatory domain

PRD-LE: PRD-like element

RdRp: RNA-dependent RNA polymerase

RF: Replicative form

RI: Replicative intermediate

RNA: Ribonucleic acid

RT-PCR: Reverse transcriptase polymerase chain reaction

SL: Stem-loop

SLEV: St. Louis encephalitis virus

STAT: Signal transducers and activators of transcription

TB: Terrific broth

TBE: Tick-borne encephalitis

TBS: Tris-buffered saline

TLR: Toll-like receptor

tRNA: Transfer RNA

Tyk: Tyrosine kinase

UTP: Uridine triphosphate

UTR: Untranslated region

VSIG: Viral stress-inducible genes

WNV: West Nile virus

YFV: Yellow fever virus

FUNCTIONAL ANALYSIS OF THE MURINE OLIGOADENYLATE SYNTHETASE 1b (*Oas1b*)

INTRODUCTION

General Characteristics of Flaviviruses

Previously part of the family *Togaviridae*, flaviviruses and pestiviruses were reclassified as part of an evolutionarily distinct family, *Flaviviridae*. The family *Flaviviridae* consists of three genera: the flaviviruses, the pestiviruses and the hepaciviruses. In addition to these genera, GB viruses have been assigned to the *Flaviviridae* family, but are not yet a genus. *Flaviviridae* belong to the positive-strand RNA virus supergroup 2, which encode similar RNA-dependant RNA polymerases (RdRp) (Lindenbach and Rice, 2001). Members of the family *Flaviviridae* share a common gene order, replication strategy, and all lack a 3' poly (A) tail.

The genus flavivirus currently contains ~70 viruses that are divided into 12 serogroups (Heinz et al., 2000), and includes a number of important human pathogens, such as yellow fever virus (YFV), dengue virus (DV), Japanese encephalitis virus (JEV), Murray Valley encephalitis virus (MVEV), St. Louis encephalitis virus (SLEV), West Nile virus (WNV), and tick-borne encephalitis (TBE). The JEV serocomplex includes JEV, MVEV, SLEV, WNV, Usutu virus, and Yaounde virus (Poidinger et al., 1996). Many flaviviruses are transmitted between vertebrate hosts by mosquitos or ticks, and as such, they are called “arboviruses” or arthropod-borne viruses. Approximately 50% of flaviviruses are transmitted by mosquitos and 28% by ticks. No known arthropod vector

has been identified for the remaining 22%, and they may be transmitted by rodent or bats (Rice, 1996; Porterfield, 1996). WNV is a mosquito-borne virus that primarily infects birds but can also infect humans (Bernard et al., 2001). West Nile virus was first isolated in Uganda in 1937 (Smithburn et al., 1940). WNV has been endemic in the Middle East, Africa, and western Asia; however, WNV recently expanded its geographical distribution to the Western hemisphere (CDC, 2003; Petersen and Roehrig, 2001).

The flavivirus genome is a single-stranded RNA of positive polarity that is involved in at least three cytoplasmic processes upon infection of the host cell: it acts as an mRNA that is used to synthesize viral proteins, it serves as a template for RNA replication, and it is targeted along with structural proteins for packaging into virions (Lindenbach and Rice, 2001). The flavivirus RNA genome contains a type I cap ($m^7GppAMP$) at the 5' terminus and is the only animal RNA virus that lacks a 3' poly (A) tail. The genomic RNA of flaviviruses encodes a single open reading frame (ORF) that is flanked by 5' and 3' untranslated regions (UTR) of about 100 and 600 nucleotides, respectively (Rice, 2001). At the end of the 3' UTR is a stem-loop structure that is absolutely required for viral replication and is highly conserved among divergent flaviviruses. A putative cyclization sequence in the 3' UTR as well as its complementary sequence in the capsid coding region of the 5' end of the genome are present in the genomes of all mosquito-borne flaviviruses (Brinton et al., 1986, You et al., 2001). A single polyprotein precursor is translated from the large ORF. The viral polyprotein is proteolytically processed by the viral serine protease (NS2B-NS3) and host cellular proteases to produce ten mature viral proteins. Three viral structural proteins, capsid (C), membrane (prM/M), and envelope (E) are encoded within the 5' part of the viral RNA

genome, while the 3' portion of the genomic RNA encodes 7 nonstructural proteins (NS1, NS2A, NS2B, NS3, NS4A, NS4B, and NS5) (Rice et al., 1985).

Molecular Biology of Flaviviruses

The flavivirus particle is small, spherical, and ~50 nm in diameter with an electron-dense ribonucleoprotein core ranging from 20 to 30 nm in diameter. A host-derived lipid envelope surrounds the flavivirus particle (Murphy, 1980). Three viral structural proteins are associated with the virion: the E, prM/M, and C proteins (Lindenbach and Rice, 2003). The mature C protein (~11 kDa) is thought to interact with viral genomic RNA in the cytoplasm to form a nucleocapsid precursor (Lindenbach and Rice, 2003); the charged residues at the N- and C- termini of the C protein presumably mediate these interactions (Khromykh and Westaway, 1996). The precursor of C, anchored C, is cleaved at its C-terminus by the viral serine protease; the C-terminal hydrophobic domain of C mediates translocation of prM to the ER prior to cleavage (Amberg et al., 1994; Lobigs, 1993; Yamshchikov and Compans, 1994). The M protein (~8 kDa) is a proteolytic fragment of its glycoprotein precursor, prM protein (~26 kDa). Late in virus maturation, during egress of the virion, prM is cleaved into mature M protein in the Golgi-network by furin, a convertase enzyme (Stadler et al., 1997). The major virion surface protein is the E protein, a glycosylated type I integral membrane protein that is ~53 kDa in size. In mature virions, E protein homodimers are arranged in a head-to-tail conformation and lie parallel to the lipid bilayer (Heinz and Allison, 2000). The E protein also forms heterodimers with prM, maintaining the E protein in a fusion-inactive conformation until virion maturation via prM cleavage and release from the cell

(Heinz and Allison, 2000). The E protein is a major antigenic determinant on the surface of flavivirus particles; it mediates cell-receptor binding and fusion during entry of the viral particle into the host cell, (Lindenbach and Rice, 2003).

Although the complete mechanism for the formation of viral RNA replication complexes has yet to be elucidated, interactions between viral nonstructural proteins and between host cell proteins and the viral proteins may be required (Brinton, 2002). NS1 is translocated to the ER and is subsequently released from the E protein by cleavage of a signal sequence recognized by a signalase (Chambers et al., 1995). The eight C-terminal residues of NS1 and ~140 N-terminal residues of NS2A are required for the cleavage of NS1 from NS2A by an unknown host protease (Chambers et al., 1990; Hori and Lai, 1990; Falgout and Markoff, 1995; Pethel et al., 1992). Although mutations that prevent cleavage at the NS1/NS2A junction have proven lethal, it is unclear what other functions are carried out by NS2A (Lindenbach and Rice, 2003). NS2B is a membrane associated protein that is required as a cofactor for the activity of the serine protease of NS3 which cleaves at multiple sites in the viral polyprotein (Chambers et al, 1991, 1993). The NS3 sequence is highly conserved among flaviviruses. Based on data demonstrating RNA-stimulated NTPase activity for the JEV NS3 (Kuo et al., 1999; Wengler and Wengler, 1991), and RNA helicase activity for the dengue 2 NS3 (Li et al., 1999), it seems likely that NS3 is also involved in RNA replication. NS5 is the viral RNA-dependent RNA polymerase and is the most conserved flavivirus protein. NS5 also contains a methyltransferase domain that may be involved in methylation of the 5' cap structure of the genomic RNA (Lindenbach and Rice, 2003; Koonin, 1993). Little is known about the roles of NS4A and NS4B; although, recent studies have suggested that they may play a

role in evading the host antiviral response by inhibition of interferon (IFN) signaling (Munoz-Jordan et al., 2003; Lin et al., 2004; Liu et al., 2004; Liu et al., 2005). For instance, Munoz-Jordan et al. (2005) suggested that the expression of NS4B of dengue-2 resulted in inhibition of signal transducers and activators of transcription-1 (STAT1) nuclear translocation in response to IFN thereby blocking the IFN signaling cascade, and that posttranslational cleavage of NS4A/NS4B by the viral protease NS3 is a prerequisite for their IFN-antagonistic properties. JEV infection blocks tyrosine phosphorylation of the cellular kinase, Tyk2, which is essential for IFN signaling (Lin et al., 2004). Several nonstructural proteins of WNV, including NS4B have been shown to inhibit STAT1/2 phosphorylation (Liu et al., 2005). West Nile virus replication prevented activation of Tyk2 and janus protein tyrosine kinase-1 (JAK) and therefore inhibited the signaling mediated by IFN- α (Guo et al., 2005).

While only short regions within the 5' UTR sequence are conserved among different flaviviruses, the 5'-terminal structure it forms shares structural homology between different flaviviruses (Brinton and Dispoto, 1988). The 3' UTR of the minus-strand, which is the site of initiation of plus-strand synthesis, is complementary to the 5' UTR. Deletions in the 5' UTR of the plus-strand proved lethal for dengue 4 replication (Cahour et al., 1995). Shi et al. (1996) detected 4 cell proteins in WNV-infected hamster cells that bind to a probe comprised of the 3' UTR of the minus-strand of WNV; TIAR and TIA-1 were subsequently identified as 2 proteins that bound to this region of WNV (Li et al, 2002). Similarly to the 5' UTR, the flavivirus 3' UTR contains only a few conserved sequences (Lindenbach and Rice, 2003). However, a 3' stem-loop (3' SL) consisting of 90 to 120 nucleotides forms a structure that is highly conserved among

divergent flaviviruses (Brinton, 1986). Specific interactions of 3 hamster cell proteins, one of which was subsequently identified as translation elongation factor 1A (EF1A), with the 3' SL of WNV RNA were reported (Blackwell and Brinton, 1995; Blackwell and Brinton, 1997).

Flaviviruses enter the host cell by receptor-mediated endocytosis after binding of the viral E protein to an unknown cell-surface receptor(s). Following cell entry, low-pH induces fusion of virion envelopes to host cell vesicle membranes in prelysosomal endocytic compartments releasing the viral nucleocapsid into the cytoplasm where the genomic RNA is uncoated by an unknown process (Lindenbach and Rice, 2003). Flavivirus infection causes significant rearrangement and proliferation of cytoplasmic, perinuclear endoplasmic reticular (ER) membranes (Brinton, 2002; Lindenbach and Rice, 2003; Knipe and Howley, 2001). The genomic RNA is translated into a single polyprotein that is cleaved at various sites by host and viral proteases to produce structural and nonstructural viral proteins (Heinz et al., 1994).

Replication of the viral RNA is thought to occur in smooth membrane vesicle clusters. However, these vesicle packets have only been observed late during infection (Mackenzie et al., 1999); thus, the site of the early events of replication is still unknown. Viral RNA replication begins by synthesis of a genome-length minus-strand RNA. The duplex formed by viral minus- and plus-strand RNAs has been termed the replicative form (RF); this RF is thought to serve as a template for synthesis of genomic RNA. The replicative intermediate (RI) contains both single and double stranded regions, presumably consisting of the minus-strand RNA template and nascent plus-strand RNAs of different lengths generated by reinitiation; this allows more than one plus-strand RNA

to be synthesized from a single minus-strand RNA at a time (Baltimore et al., 1968; Wengler et al., 1978; Cleaves and Dubin, 1979; Cleaves et al., 1981; Chu and Westaway, 1985). Although negative-strands continuously accumulate during infection, they have been isolated in double-stranded forms only (Cleaves et al., 1981; Wengler et al., 1978). The observed 10- to 100-fold excess of viral plus-strand RNAs over negative-strand RNAs in infected cells has been attributed to a semiconservative and asymmetric mode of replication (Cleaves et al., 1981; Chu and Westaway, 1985). Little is known about viral packaging and release, although viral assembly occurs in association with rough ER membranes (Lindenbach and Rice, 2003). Accumulation of intracellular immature virions in vesicles is followed by transport through the host secretory pathway where the N-terminal portion of prM is cleaved in the Golgi-apparatus (Wengler, 1989; Stadler et al., 1997). As the new virions are transported to the plasma membrane in vesicles, they are released by exocytosis (Mason, 1989).

Genetic resistance to flavivirus-induced disease

Interactions between host-specific factors and viral components influence the course and outcome of flaviviral infections (Bang, 1978). Observations of flavivirus infections in horses, birds, rodents, humans, and non-human primates, suggest an innate resistance to flavivirus-induced disease in some individuals from a number of species (Shellam et al., 1998). Horses infected with WNV showed differential susceptibility to WNV-induced disease (Bunning et al., 2002; Durand et al. 2000). Challenge of 4 species of grouse with louping ill (LI) virus (a flavivirus) showed that three of the species (red grouse, willow grouse, and ptarmigan) developed high levels of viremia and died. The

fourth species (capercaillie) had very low levels of viremia and survived (Reid et al., 1980). Similarly, yellow fever virus infection has been shown to be clinically mild in African species of monkeys, while usually deadly in South American species of monkeys (Shellam et al., 1998; Bauer and Mahaffy, 1930; Smithburn and Haddow, 1949). Observations during two dengue virus epidemics in Cuba in 1981 and 1997 showed that fewer blacks were hospitalized with dengue hemorrhagic fever/dengue shock syndrome than whites suggesting the presence of a dengue resistance gene and that more blacks than whites carried the resistant allele(s) (Kouri et al., 1987; Kouri et al., 1989; Guzman et al., 1990). In 2002 in the Chicago area, 52 % of the population consisted of white individuals but whites accounted for ~83 % of the individuals showing symptoms of WNV-induced disease (Ruiz et al., 2004). Although no resistance gene against flavivirus-induced has yet been found in humans yet, a single gene in mice (*Flv*) has been shown to affect the levels of virus production and the severity and outcome of disease caused by flaviviruses (reviewed in Brinton, 1986).

Murine resistance to flavivirus-induced disease

Leslie Webster, in the 1920's, established strains of mice that were either resistant or susceptible to paratyphoid (bacterial) infection through selective breeding (Webster, 1923). Mouse strains resistant and susceptible to louping ill virus were also established (Webster, 1933). Independent segregation of bacterial and viral resistance was demonstrated by establishment of mouse strains that showed resistance to only one type of infection, either paratyphoid or louping ill virus infection but not both. Resistant mice that survived louping ill virus challenge were later shown to be resistance to SLEV, a

mosquito-borne virus, and Russian spring-summer virus, a tick-borne virus (Webster, 1937; Casals and Schnider, 1943). Subsequently, infection of the mice with a number of different viruses showed that although resistance was conferred against both mosquito- and tick-borne flaviviruses, resistance did not extend to other types of viruses (Brinton and Pereygin, 2003; and references therein). Monogenic, autosomal inheritance was shown for the flavivirus resistance phenotype (Sabin, 1952). Production of a congenic flavivirus-resistant C3H/RV strain was accomplished by the introduction of the resistance gene carried by PRI mice into the flavivirus-susceptible C3H/He strain (Groschel and Koprowski, 1965). The C3H/RV strain was subsequently renamed C3H.PRI.*Flv^r* (Urosevic et al., 1999).

Although resistant mice are resistant to disease induced by all flaviviruses tested, they are susceptible to flavivirus infection. A number of factors such as route of inoculation, dose and virulence of the infecting virus can all influence the outcome of flavivirus infection in mice. For instance, C3H.PRI.*Flv^r* mice show complete resistance to intracerebral inoculation of YFV-17D vaccine, whereas intracerebral inoculation by the more virulent WNV can kill the resistant mice. Nevertheless, intracerebral inoculation with 50,000 PFU of WNV resulted in 33 % mortality in resistant mice, compared to 82 % mortality in susceptible ones after a 5,000 PFU intracerebral inoculation of WNV (Brinton Darnell et al., 1974). Intraperitoneal injection of $10^{8.5}$ PFU WNV did not cause disease in resistant mice, while 50 % mortality was achieved in susceptible mice after injection of $10^{7.5}$ PFU of WNV intraperitoneally (Brinton, 1986). Resistant mice produced much lower titers of flavivirus, and showed a slower spread of infection as compared to congenic susceptible C3H/He mice (Shellam et al., 1998;

Goodman and Koprowski, 1962; Brinton Darnell et al., 1974; Brinton Darnell and Koprowski, 1974; Webster and Johnson, 1941; Vainio, 1963). Henson et al. (1969) demonstrated that peak brain titers are 10,000 fold lower in resistant mice compared to susceptible mice after a $10^{5.5}$ PFU intracerebral inoculation of WNV; and that peak titers were observed by day 3, with death on day 4, in susceptible mice and day 4, with death on day 7 or 8 in resistant mice.

Intraperitoneal challenge with Banzi virus was lethal in C3H.PRI.*Flv'* mice that were younger than 4 weeks old and full resistance was not achieved until the mice reached 8 to 12 weeks (Bhatt and Jacoby, 1976). Suppression of the immune system which prevented production of antiviral antibodies or T cells during Banzi virus infection proved deleterious for both resistant and susceptible mice; suggesting an important role for a mature and intact immune system in clearing flavivirus infection (Bhatt and Jacoby, 1976). Intracerebral inoculation of resistant mice with YFV-17D after injection with anti-IFN antibodies showed no difference in their *Flv'* phenotype, illustrating that flavivirus resistance is not mediated by interferon (Brinton et al., 1982).

WNV infection of primary cell cultures prepared from embryofibroblasts derived from resistant and susceptible mice produced virus titers that differed by 10 to 100-fold (Brinton Darnell and Koprowski, 1974). Interestingly, analysis of viral RNA produced in embryofibroblast cultures from resistant and susceptible mice at very early times after WNV infection showed that there were significantly lower amounts of plus-strand RNA in the resistant cells than in the susceptible cells; both types of cells had the same amount of negative-strand RNA (Brinton, 1981).

Virus stress-induced genes

Viral stress-inducible genes (VSIG) consist of a common set of genes that are inducible by viral infection, dsRNA and interferons (IFN). Stresses caused by viral infection result in a strong and transient induction of these genes (Sarkar and Sen, 2004). Although VSIG were initially discovered as IFN-inducible genes, they are capable of being induced in an IFN-independent manner (Daly and Reich, 1993; Bandyopadhyay et al., 1995; Weaver et al., 1998). Interestingly, microarray data suggest that the same VSIG may be induced via different signaling pathways depending on the inducer (Der et al., 1998; Zhu et al., 1998; Chang and Laimins, 2000; Geiss et al., 2001; Johnston et al., 2001; Mossman et al., 2001; Geiss et al., 2002; Geiss et al., 2003). The IFN-stimulated response element (ISRE) is a *cis*-acting sequence present in the promoters of all of these genes.

Interferons are divided into type I and type II, and both types have antiviral activity (Biron and Sen, 2001; Samuel, 2001; Finter, 1996). Both types of interferon are structurally unrelated and their actions are mediated by different and structurally unrelated cell-surface receptors (Sarkar and Sen, 2004). The type I IFN family includes IFN- α , IFN- β , IFN- ω and IFN- τ ; while IFN- γ is the only known type II interferon (Sarkar and Sen, 2004). A positive regulatory domain (PRD) and a PRD-like element (PRD-LE) are *cis*-acting elements present in the promoters of IFN- α and IFN- β , respectively; these elements are inducible by interferon regulatory factors (IRFs) (Nakaya et al., 2001; and references therein). The IRF-family transcription factors bind to the PRD/PRD-LEs and ISREs present in the promoters of IFN and ISGs to induce the transcription of more than a 100 genes involved in the antiviral signaling pathways, either IFN-dependent or

independent (Nakaya et al., 2001). The prerequisite for Toll-like receptor 3 (TLR3), but not other TLRs, for activation of dsRNA mediated gene induction was demonstrated in dsRNA-unresponsive 293 cells that respond to dsRNA in the presence of exogenous TLR3 and not other TLRs (Alexpoulou et al., 2001). The presence of viral dsRNA in infected cells elicits phosphorylation of the cytoplasmic domain of TLR3 which leads to activation of IRF3, which is constitutively expressed, via adaptor proteins (Jiang et al., 2004). Once phosphorylated, IRF3 dimerizes and is then translocated to the nucleus where it may form a complex with CBP and p300 forming double-stranded RNA-activated factor 1 (DRAF1) (Daly and Reich, 1995; Weaver et al., 1998). DRAF1 can bind to ISREs in promoter regions of ISGs to activate transcription of genes such as ISG15 and ISG54; DRAF1 also binds to PRD in the IFN- β promoter, inducing transcription of IFN- β (Juang et al., 1998; Lin et al., 1998; Sato et al., 1998b; Wathelet et al., 1998; Yoneyama, et al., 1998). IFN produced in the infected cell is secreted and binds to receptors on the surface of both infected cells and surrounding uninfected cells. IFN binding to the IFN- α /b receptor (IFNAR) causes cross-activation of Jak1 and Tyk2, which phosphorylate one another along with STAT1 and STAT2. The phosphorylated STATs form IFN stimulated gene factor 3 (ISGF3), a trimeric complex including STAT1, STAT2 and IRF9. The ISGF3 complex translocates to the nucleus where it binds to ISREs in promoter regions to activate transcription of ISGs such as PKR, OAS family members and IRF7 (Darnell et al., 1994; Stark et al., 1998; Nakaya et al., 2001). Once phosphorylated due to viral dsRNA, IRF7 moves to the nucleus to further activate IFN α / β promoters resulting in massive IFN α / β production that is maintained via a positive feedback loop (Nakaya et al., 2001; Marie et al., 1998; Sato et al., 1998a; Au et al., 1998).

Gene induction by dsRNAs may be mediated by TLR3 and INF-independent pathways. The protein kinase RNA regulated (PKR) protein contains two dsRNA-binding motifs (dsRBM) at its N-terminus; when inactive, the dsRBM2 of PKR binds the C-terminal kinase domain (Clemens and Elia, 1997). PKR is in the inactive and closed conformation until it interacts with dsRNA which causes the release of the kinase domain from dsRBM2 allowing ATP binding resulting in autophosphorylation and activation (Nanduri et al., 2000). Kumar et al. (1997) suggested the presence of a PKR-independent mechanism of dsRNA signaling using PKR knock-out (PKR^{-/-}) fibroblasts. Such a mechanism may involve members of the 2'-5' oligoadenylate synthetase (OAS) family of proteins which have been shown to be activated in the presence of dsRNA and ATP, leading to degradation of viral and cellular RNAs by RNase L (Hovanessian, 1991; Lengyel, 1987; Silverman and Cirino, 1997).

Chromosomal mapping and identification of the *Flv'* gene

Different alleles for natural resistance to *Rickettsia tsutsugamushi*, which causes experimental scrub typhus in mice, were discovered in C3H/He and congenic C3H.PRI.*Flv'* mice at the *Ric* locus on chromosome 5. C3H/He mice carry the *Ric*^s (susceptible) allele, and C3H.PRI.*Flv'* mice carry the *Ric*^r (resistant) allele (Groves et al., 1980; Jerrells and Osterman, 1981). A second locus tightly linked to *Ric* was subsequently identified on chromosome 5 as *rd* (Lyon and Kirby, 1993). C3H/He mice carry a recessive, defective allele of this gene, which causes retinal degeneration, while the C3H.PRI.*Flv'* mice carry wild-type *rd* (Bowes et al., 1990; La Vail and Sideman, 1974). The differences in the *Ric* and *rd* loci in the two mouse strains seemed to

segregate with the *Flv^r* gene and the fact that these strains of mice are congenic, suggested that the *Flv^r* gene was linked to these two genes. Three-point backcross linkage analyses using 4 chromosome 5 markers, *Pgm-1*, *Eta-1* (*Ric* synonym), *rd*, and *Gus-s* (glucuronidase structural gene), showed the gene order was *Pgm-1*, *Eta-*, *rd*, *Flv^r* and *Gus-s* (Sangster et al., 1994; Shellam et al., 1993). Based on mapping data obtained by Urosevic et al. (1997), it was estimated that the *Flv* gene and the *DMit159* microsatellite were less than 0.15 centiMorgans (cM) apart on mouse chromosome 5 (Perelygin et al., 2002). The distance was approximately equivalent to 309 kb and it was highly likely (>95 %) that this distance downstream and upstream of the *DMit159* microsatellite would contain the *Flv* locus (Perelygin et al., 2002). Twenty-two genes, including 10 loci that encoded 2'-5' oligoadenylate synthetases, were identified (Perelygin et al., 2002). The cDNAs from each of the 22 genes in this region from both C3H.PRI.*Flv^r* and C3H/He strains were amplified by RT-PCR, sequenced and compared. Of the 22 gene sequences compared, only *Oas1b* and the Na⁺/Ca⁺-exchanger were polymorphic; however the Na⁺/Ca⁺-exchanger was ruled out as there was no consistent correlation between polymorphisms in this gene and the resistant phenotype (Perelygin et al., 2002). The genomic and cDNA sequences of *Oas1b* revealed that the gene contained 6 exons and that 4 resistant mouse strains (BRVR, CASA/Rk, Cast/Ei, and C3H.PRI.*Flv^r*) encode an identical full-length protein; whereas in 5 susceptible mouse strains (129/SvJ, BALB/c, C57BL/6, CBA/J and C3H.PRI.*Flv^r*) an identical truncated protein was encoded due to a C820T transition (Perelygin et al., 2002). The truncation of the *Oas1b* protein was consistently correlated with the susceptible phenotype (Perelygin et al., 2002).

The *Flv* gene was identified as 2'-5' oligoadenylate synthetase 1b, Oas1b (Perelygin et al., 2002). The resistant allele was designated *Flv^r*, and encodes a full-length Oas1b protein. The susceptible allele was designated *Flv^s*, and encodes a C-terminally truncated protein that also has two amino acid substitutions as compared to the *Flv^r* product. The minor resistance allele was designated *Flv^{mr}* (Sangster et al., 1993), and encodes a full-length Oas1b protein that has 14 amino acid substitutions as compared to the *Flv^r* product (Perelygin et al., 2002).

The 2'-5' oligoadenylate synthetase family

Humans, horses, mice and other mammals produce 3 types of 2'-5' oligoadenylate synthetases: small encoded by the Oas1 gene(s), medium encoded by the Oas2 gene and large encoded by the Oas3 gene. Two Oas-like proteins that contain C-terminal ubiquitin-like domains are also produced. The Oas1 unit consists of N- and C-terminal domains that are unique to the 2'-5' oligoadenylate synthetase family and contains a central domain with a nucleotidyltransferase fold. The Oas2 and Oas3 genes consist of 2 and 3 Oas1 gene units, respectively. The Oas-like genes consist of the homologous N-terminus but contain a C-terminal ubiquitin-like domain (Hartmann et al, 1998). In humans, genes in the family are designated OAS, unlike in mice where they are designated Oas. The human OAS genes are located on chromosome 12, while in horses they are located on chromosome 8 and in mice they are located on chromosome 5 (Perelygin et al., 2004). Recently, Hartmann et al (2003) reported the crystal structure of the porcine OAS1 as a monomeric protein that is bilobal in structure. The first lobe of the protein encompasses the large catalytic domain that is connected to the C-terminal

domain by a helix-loop-helix linker. The N-terminus forms a short hook that packs against the C-terminal domain to form a tether that maintains a fold which would allow the domain-domain interactions that are required for enzymatic activity. The structure formed has a negatively charged cleft containing the active site. Parallel to the cleft and on the back face of the structure is a groove composed of positively charged residues in which dsRNA is thought to bind. Binding of the dsRNA may cause a conformational change that widens the cleft of the protein to allow recruitment of the substrate ATP which then leads to the synthesis of 2'-5' oligoadenylates (Hartmann et al., 2003). The human OAS1 and the mouse Oas1a and Oas1g are functionally active 2'-5' oligoadenylate synthetases. The human hOASL and its murine ortholog mOas1l are not functionally active, while the mouse mOas2 was shown to be a functionally active synthetase (Eskildsen et al., 2003).

Murine Oligoadenylate Synthetases

Mice produce 3 types of 2'-5' oligoadenylate synthetases, small (40-47 kDa) encoded by the Oas1a-Oas1h genes, medium (85-86 kDa) encoded by the Oas2 gene, and large (126 kDa) encoded by the Oas3 gene. Mice also produce two Oas-like proteins. The small 2'-5' oligoadenylate synthetases contain 3 functional motifs; an N-terminal LXXXP motif required for 2'-5' oligoadenylate synthetase activity, a P-loop motif that has been suggested to be required for ATP-binding, and a DAD Mg²⁺ binding motif also required for synthetase function. Active 2'-5' oligoadenylate synthetases bind double-stranded RNA and some double-stranded regions within folded single-stranded RNA (Maitra et al., 1998; Desai et al., 1995; Sharp et al., 1999) and produce 2'-5'

oligoadenylate by polymerizing ATP through 2'-5' linkages. One cellular defense mechanism involves the activation of a latent endoribonuclease called RNase L. 2'-5' oligoadenylates produced by activated 2-5A synthetases activate RNase L. Once activated, RNase L dimerizes and degrades viral and cellular single-stranded RNAs after UA and UU dinucleotides (Wreschner, et al. 1981). Although the functions of 2'-5' oligoadenylates and RNase L are virus non-specific (Hovanessian and Wood, 1980; Clemens and Williams, 1978), the antiviral effect of the Oas1b gene product is specific to members of the flavivirus genus (Perelygin et al., 2002).

Goals of the project

Resistance to flavivirus-induced disease was demonstrated in mice and showed monogenic autosomal dominant inheritance. The flavivirus resistance gene, *Flv*, in mice has been identified as 2'-5' oligoadenylate synthetase 1b (Oas1b). Susceptible mice produce a protein that is truncated (Oas1btr) at the C-terminus due to a premature stop codon encoded by a C820T transition. The truncation comprises 30 % of the C-terminus of the protein. Mice produce 8 Oas1 proteins, Oas1a-Oas1h. Oas1a and Oas1g were previously reported to be functional 2-5A synthetases. Poly (I:C) binding was also reported for Oas1a, Oas1c, Oas1d, Oas1e, Oas1f, Oas1g, Oas1h and Oas1btr proteins (Kakuta et al., 2002). The full-length Oas1b had not yet been tested for either 2-5A synthetase activity or RNA binding activity. The first goal of this project was to express Oas1a, Oas1b and Oas1btr in bacteria and to purify the expressed proteins. The second goal was to test the expressed Oas1 proteins for 2-5A synthetase activity to determine whether Oas1b had synthetase activity. The final goal of the project was to test the ability of the expressed Oas1 proteins to bind to synthetic and viral RNAs.

MATERIALS AND METHODS

Cloning of Oas1 proteins into pMAL-c2G vectors: pHeTopoXL1a, previously constructed by Dr. Perelygin, and primers containing the SnaBI and BamHI restriction sites were used to clone the Oas1a gene into pCR-XL-TOPO with the TOPO-TA cloning kit (Invitrogen). The construct was named pTopoXL1a#10. pTopoXL1a#10 and pMAL-c2G vector DNAs were digested with SnaBI and BamHI. The digestion was done sequentially; briefly, pTopoXL1a#10 and pMAL-c2G DNAs were each digested with BamHI and then QIAGEN's PCR purification protocol was used to purify the DNA. The cut pTopoXL1a#10 and pMAL-c2G DNAs were digested with SnaBI. The reactions were then electrophoresed on a 1% TBE agarose gel. The vector and the 1101 bp Oas1a gene insert were isolated using the QIAGEN Gel Extraction protocol.

pScreen1b#18, previously constructed by Dr. Scherbik, and primers containing the SnaBI and BamHI restriction sites were used to clone the full-length Oas1b gene into pCR-XL-TOPO by using the TOPO-TA cloning kit (Invitrogen). The construct was named pTopoXL1b#1. pTopoXL1b#1 and pMAL-c2G vector DNAs were digested with SnaBI and BamHI. The digestion was done sequentially; briefly, pTopoXL1b#1 and pMAL-c2G DNAs were each digested with BamHI and then QIAGEN's PCR purification protocol was used to purify the DNA. The cut pTopoXL1b#1 and pMAL-c2G DNA were digested with SnaBI. The reactions were then electrophoresed on a 1% TBE agarose gel. The vector and the 1128 bp Oas1b gene insert were isolated using the QIAGEN Gel Extraction protocol.

Using the TOPO-TA cloning kit (Invitrogen), pTopoXL1btr#2, which contained the Oas1btr gene, was constructed by using pTopoXL1b#1 as a template along with

primers containing the SnaBI and BamHI. The BamHI-containing primer also encoded a C-T transition in the Arg codon at position 757 resulting in a stop codon. pTopoXL1btr#2 and pMAL-c2G vector DNAs were digested with SnaBI and BamHI. The digestion was done sequentially; briefly, pTopoXL1btr#2 and pMAL-c2G DNAs were each digested with BamHI and then QIAGEN's PCR purification protocol was used to purify the DNA. The cut pTopoXL1btr#2 and pMAL-c2G DNAs were digested with SnaBI. The reactions were then electrophoresed on a 1% TBE agarose gel. The vector and the 756 bp Oas1btr gene insert were isolated using the QIAGEN Gel Extraction protocol.

The vectors and inserts were ligated using T4 DNA ligase according to a modified protocol. Briefly, the vector and insert DNAs were heated to 45°C for 5 minutes and cooled on ice prior to addition of the T4 DNA ligase. The ligation reaction was incubated at 16°C overnight. The reaction was then heated to 65°C to inactivate the ligase and cooled on ice. The ligation reaction was then transformed into TOP10 One Shot Chemically competent cells and plated on LB + AMP plates. The transformation was modified to include two minutes of heat-shocking the competent cells and a longer incubation than usual. PCR screening was performed on the colonies using primers specific to the insert. The colonies were cultured and plasmid miniprep kits were used to isolate plasmids from the cells. After isolating the plasmids, a sequencing reaction was run on each plasmid using malE forward and M13/pUC reverse primers to check the sequence.

Expression of MBP-Oas1 Proteins: pMAL-O1aQCR was used to transform BL21 (non-D3E) cells for the expression of recombinant Oas1a (MBP-Oas1a) protein.

Five mls of culture were grown overnight at 37°C. The 5 mls of overnight culture was added to 250 mls of Rich Media with 0.05% glucose and 75 mg/ml of carbenicillin (CRB) and grown at 37°C until the culture reached an OD₆₀₀ of ~0.75. Two 1 ml samples were collected and centrifuged at 14,000 x g for 2 minutes. The supernatant was removed and the pellet was resuspended in 100 µl of 2x SDS buffer with 5 % β-mercaptoethanol (β-ME); this was the uninduced sample. The rest of the culture was induced with 1 mM IPTG overnight at 16°C. Two 1 ml samples were collected from the overnight-induced culture and centrifuged at 14,000 x g for 2 minutes. The supernatant was removed and the pellet was resuspended in 100 µl of 2x SDS buffer with β-mercaptoethanol; this was the induced sample. The rest of the culture was pelleted by centrifugation at 5,000 x g for 15 minutes. The supernatant was removed and resuspended in 5 ml of column buffer (20 mM tris-HCl, 200 mM NaCl, 1 mM EDTA and 10 mM β-ME) and frozen at -20°C until use.

pMAL-O1b was used to transform BL21 (nom-DE3) cells for expression of recombinant Oas1b (MBP-Oas1b) protein. Five mls of culture were grown overnight at 37°C. The 5 mls of overnight culture was added to either 500 mls of TB Autoinduction media (Novagen) with 0.05% glucose and 75 mg/ml of carbenicillin (CRB), or 500 mls of LB media with 0.05% glucose and 75 mg/ml of carbenicillin (CRB); cultures were grown at 37°C until the culture reached an OD₆₀₀ of ~0.6. Two 1 ml samples were collected and centrifuged at 14,000 x g for 2 minutes. The supernatant was removed and the pellet was resuspended in 100 µl of 2x SDS buffer with 5 % β-ME; this was the uninduced sample. The rest of the culture was either induced with 0.5 mM IPTG in LB or allowed to grow for auto-induction without IPTG overnight at 16°C. Two 1 ml

samples were collected from the overnight-induced culture and centrifuged at 14,000 x g for 2 minutes. The supernatant was removed and the pellet was resuspended in 100 µl of 2x SDS buffer with 5 % β-ME; this was the induced sample. The rest of the culture was pelleted by centrifugation at 5,000 x g for 15 minutes. The supernatant was removed and resuspended in 3 ml of column buffer and frozen at -20°C until use.

pMAL-O1btr was used for the expression of recombinant Oas1btr (MBP-Oas1btr) protein in BL21 (non-D3E) bacterial cells. Five mls of culture were grown overnight at 37°C. The 5 mls of overnight culture were added to 250 mls of Rich media with 0.05% glucose and 75 mg/ml of carbenicillin (CRB) and grown at 37°C until the culture reached an OD₆₀₀ of ~0.5. Two 1 ml samples were collected and centrifuged at 14,000 x g for 2 minutes. The supernatant was removed and the pellet was resuspended in 100 µl of 2x SDS buffer with 5 % β-ME; this was the uninduced sample. The rest of the culture was induced with 0.5 mM IPTG overnight at 16°C. Two 1 ml samples were collected from the overnight-induced culture and centrifuged at 14,000 x g for 2 minutes. The supernatant was removed and the pellet was resuspended in 100 µl of 2x SDS buffer with 5 % β-ME; this was the induced sample. The rest of the culture was pelleted by centrifugation at 5,000 x g for 15 minutes. The supernatant was removed and resuspended in 5 mls of column buffer and frozen at -20°C until further use.

Purification of MBP-Oas1 protein: The Oas1 recombinant proteins were successfully purified by column purification using amylose resin. Cultures for the expression of MBP-Oas1a, MBP-Oas1b and MBP-Oas1btr were prepared as described above. The cultures were pelleted and the cells were resuspended in column buffer and lysed using a French press.

The soluble fraction (crude) and insoluble fraction were separated by centrifugation at 10,000 x g for 20 minutes. The crude sample was diluted 1:5 in column buffer and loaded onto a 2.5 cm x 10 cm column that contained 2 ml of equilibrated amylose resin. The sample was allowed to flow through the column, collected and reloaded onto the column three times to ensure that the protein efficiently bound to the resin. The resin was washed with 100 ml of column buffer, and the MBP-fusion protein was then eluted from the column with 10 mM maltose in column buffer.

Alternatively, the Oas1 proteins were purified using ion exchange chromatography by loading the crude sample onto an anion exchange column (HiTrap Q HP). The proteins in the samples were separated by a salt gradient. Buffer A is 20 mM Tris-HCl, pH 7.6 and buffer B is 20 mM Tris-HCl, pH 7.6 and 1M NaCl. The MBP-Oas1a protein was eluted between concentrations of 550 mM and 800 mM NaCl. The MBP-Oas1b protein was eluted between concentrations of 600 mM and 750 mM NaCl. The MBP-Oas1btr protein was eluted between concentrations of 500 mM and 750 mM NaCl. The protein concentrations obtained using the FPLC were very low and had to be concentrated 100-fold to be visualized after SDS-PAGE.

Cleavage of the MBP fusion: In a reaction tube, 5.5 μ l of Genenase I (1 μ g/ μ l) was added to 520 μ l of MBP-Oas1a (600 ng/ μ l) and incubated at room temperature. Five μ l samples were taken from the digestion reaction at 2, 4, 24 and 28 hours. In a separate tube, 5 μ l of fusion protein were incubated for 28 hours; this was the mock digestion sample. Five μ l of fusion protein were mixed with 2X SDS gel-loading buffer with 5 % β -ME at the end of the digestion period; this was the uncut fusion sample. Each sample

was mixed with 2X SDS gel-loading buffer containing 5 % β -ME, boiled for 5 minutes and stored at 4°C until analyzed. Samples were electrophoresed on a 10 % SDS-PAGE.

Separation of Oas1a from MBP by hydroxyapatite chromatography: One g of hydroxyapatite was reconstituted in buffer C [20 mM sodium phosphate, 200 mM NaCl (pH 7.2)]. The resin was allowed to settle and excess buffer was carefully decanted as to not disturb the resin. Fresh buffer was added and this process was repeated twice. The hydroxyapatite was poured into a disposable 1 x 10 cm column (BD Clontech). Five hundred μ l of the fusion protein cleavage mixture was loaded onto the column. The column was washed with 80 ml of buffer C to wash away the maltose. Twenty ml of 0.5 M sodium phosphate (pH 7.2) were used to elute the Oas1a protein, the MBP fusion and the protease. The column was reloaded twice more to ensure complete elution of protein. The eluate was then loaded onto an amylose column. The flow-through was collected and reloaded twice more to increase the efficiency of binding of the MBP fusion fragment to the amylose resin. The flow-through was concentrated to 450 μ l and stored at -80°C until use.

Western blotting: MBP-Oas1 proteins were separated under denaturing and reducing conditions on a 10 % SDS-PAGE. The proteins were transferred to a PVDF membrane and the membrane was blocked overnight at 4°C with 5 % bovine serum albumin (BSA) in Tris-buffered saline [10 mM Tris-HCl (pH 8.0), 150 mM NaCl] (TBS).

A horseradish peroxidase (HRP) conjugated anti-MBP (monoclonal murine anti-MBP, New England Biolabs) antibody was used to detect the MBP-Oas1 proteins. The membrane was incubated with antibody diluted 1:35,000 in a 5 % BSA-TBS solution at

room temperature for 1.5 hrs. The membrane was washed with 15 ml of a 0.05 % Tween-20-TBS solution (TBS-T) for 15 minutes 6-8 times.

For detection of the Oas1a protein after cleavage of MBP, an anti-OAS1 antibody (chicken anti-human-OAS1 IgY, Genway Biotech) was used. The membrane was incubated with anti-OAS1 antibody diluted 1:2,000 in a 5 % BSA-TBS solution at room temperature for 1.5 hrs. The membrane was washed with 15 ml of TBS-T for 15 minutes 6-8 times. The membrane was then incubated with a HRP-conjugated goat anti-IgY Fc (Genway Biotech) antibody diluted 1:3,000 in a 5 % BSA-TBS-T solution at room temperature for 1.5 hrs. The membrane was washed with 15 ml of TBS-T for 15 minutes 6-8 times.

After the last wash, West Pico Enhanced Chemiluminescence reagent (Pierce) was added to the membrane for 5 minutes at room temperature. The membrane was exposed with autoradiography film.

2'-5' Oas activity assay: MBP-Oas1 fusion proteins were assayed for 2'-5' Oas activity. Each of the MBP-Oas1 fusion proteins was added to reaction mixtures at increasing concentrations. The 50 μ l reaction mixture contained 2'-5' OAS activity assay buffer (20 mM HEPES-KOH pH 7.5, 50 mM KCl, 25 mM Mg(OAc)₂, 10 mM creatine phosphate, 1U/ μ l creatine kinase, 5 mM ATP, and 7 mM β -ME), 50 μ g/ml poly (I:C), 10 μ Ci ³²p-ATP. The reaction was incubated at 30°C for 18 hrs. The synthesis reaction was stopped by addition of 50 μ l of 2x gel loading buffer (95% formamide, 18 mM EDTA, 0.025% SDS, xylene cyanol, and bromophenol blue). Four μ l of each reaction were loaded onto a 20% polyacrylamide gel and electrophoresed at 1800 V for 3.5 hrs. The gel was exposed to an autoradiography film for 1-24 hrs.

Synthesis of RNA probes: Three probes were constructed to test the ability of the MBP-Oas1 fusion proteins to bind dsRNAs. The first probe, designated 3' (+) UA Probe #1, encompassed nucleotides 10387-10448 of the WNV Eg101 genome. The second probe, designated 3' (+) Control Probe #2, encompassed nucleotides 10308-10364 of the WNV Eg101 genome. The third probe, designated 3' (+) SL Probe #3, encompassed bases 10931-11029 of the WNV Eg101 genome. The probes were synthesized using the *in vitro* T7 RNA polymerase MAXIscript protocol (Ambion) in the presence of radiolabeled UTP (³²p-UTP). The RNA transcripts were gel-purified and partially purified by precipitation.

Gel electrophoresis mobility shift assay: The binding activity of each of the MBP-Oas1 fusion proteins was tested by gel mobility shift assay using various RNA probes from the 3' end of the WNV genome. Proteins were added into binding reactions containing 1X Gel Shift Buffer (3% Ficoll-400, 20 mM sodium phosphate pH 7.2, 60 mM KCl, 1 mM MgCl₂, and 0.5 mM EDTA), 0.2 ul of RNasin, 35 ng of yeast tRNA as non-specific competitor, 10 mM (DTT) dithiothreitol, and radiolabeled RNA. Reactions were incubated at room temperature for 20 minutes and then stopped by the addition of gel loading buffer (0.025% bromophenol blue, 0.025% xylene cyanol, 4% sucrose, and 1X Tris borate-EDTA). The reactions were electrophoresed on non-denaturing 5% polyacrylamide gels (39:1 acrylamide:bis-acrylamide, and 1X Tris borate-EDTA) at 120 V for 2 hrs. at 4°C. The gel was then dried and analyzed with a PhosphorImager.

RESULTS

Cloning and expression of MBP-Oas1 proteins in bacteria

Initial attempts to express the full-length Oas1b protein using a pET16b expression vector (Novagen) yielded proteins that were insoluble and were mainly in inclusion bodies. The concentrations of expressed proteins were inadequate for purification. The expressed protein contained a 10X histidine tag at the N-terminus. The use of different strains of bacteria and different growth and induction conditions failed to alleviate the problems encountered with expression using the pET system (data not shown). As a result, the pMAL Protein Fusion and Purification System was subsequently used to express soluble Oas1b proteins that were fused to maltose binding protein (MBP). Recombinant proteins expressed using the pMALc2G vector contained the MBP fusion at the N-terminus and were soluble.

The cDNAs of the full-length and truncated Oas1b proteins as well as of the Oas1a protein were each cloned into the pMAL-c2G expression vector. The expressed fusion protein consisted of a 42.5 KDa maltose-binding protein linked to the Oas1 protein by 10 Asp residues. Each of the constructs was used to express recombinant Oas protein in BL21 bacterial cells. Cultures were grown at 37°C until an OD₆₀₀ of approximately 0.6 was reached. The cultures were induced with IPTG overnight at 16°C. Samples were collected and resuspended in 100 µl of 2X SDS gel loading buffer. Expression of the fusion proteins was analyzed by electrophoresis of 15 µl from each sample on a 10 % SDS polyacrylamide gel (**Fig. 1**).

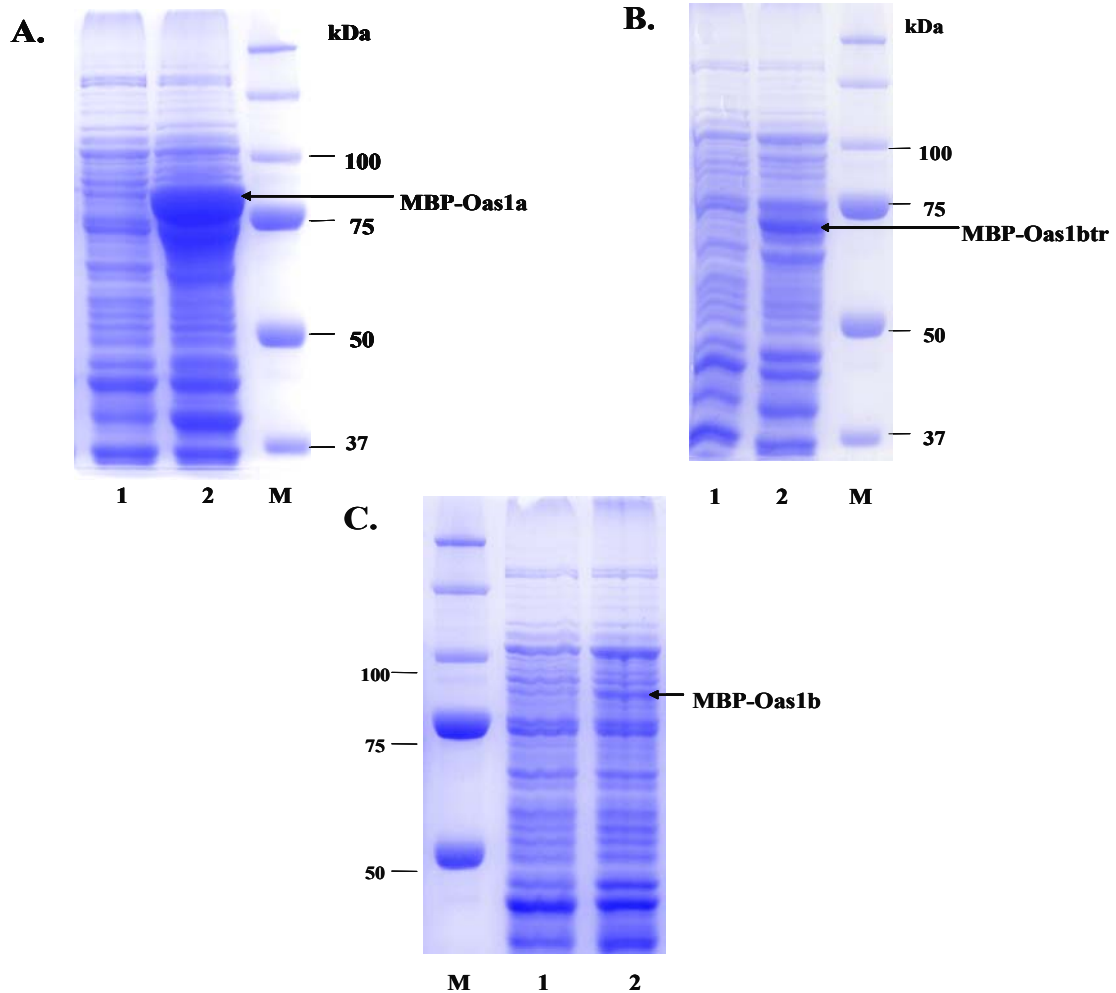


Figure 1: Expression of Oas1a, Oas1b and Oas1btr proteins in bacteria. Total proteins were separated by 10% SDS-PAGE. **(A)** Expression of MBP-Oas1a in BL21 (non-DE3) cells. **Lane 1:** Uninduced cells. **Lane 2:** Cells induced with 1mM IPTG overnight at 16°C. **(B)** Expression of MBP-Oas1btr in BL21 (non-DE3) cells. **Lane 1:** Uninduced cells. **Lane 2:** Cells induced with 1mM IPTG overnight at 16°C. **(C)** Expression of MBP-Oas1b in BL21 (non-DE3) cells. **Lane 1:** Uninduced cells. **Lane 2:** Cells induced with 0.5mM IPTG overnight at 16°C. **M:** Molecular weight markers, Precision Plus protein standards (Bio-Rad).

Interestingly, the expression of MBP-Oas1a was more efficient than that of MBP-Oas1b and MBP-Oas1btr; also, the observed expression level of MBP-Oas1btr was noticeably higher than that of MBP-Oas1b.

Purification of MBP-Oas1 fusion proteins

MBP-Oas1 fusion proteins were purified from cultures of BL21 bacterial cells. Each of the expressed fusion proteins was soluble (**Fig. 2A lane 3, Fig. 2B lane 3, Fig. 2C lane 1**). Cell pellets from induced cultures were resuspended in column buffer containing protease inhibitor cocktail to minimize protein degradation and all purification steps were carried out at 4°C. The cells were lysed by using a French press and the suspension was clarified by centrifugation. MBP-Oas1 fusion proteins were purified using amylose resin as described in Methods. Protein eluted from the resin was concentrated by using Centricon YM-30 concentrators (Millipore) and separated by 10 % SDS-PAGE.

MBP-Oas1a, MBP-Oas1b, and MBP-Oas1btr were successfully purified by amylose resin column purification (**Fig. 2A lanes 7 and 8, Fig. 2B lanes 6-8; Fig. 2C lane 1**). MBP-Oas1btr was initially purified by chromatography on an anion exchange column (HiTrap Q HP) as described in Methods (**Fig. 2D**). Although extremely pure, the amount of MBP-Oas1btr recovered using this method was not sufficient for experimentation. MBP-Oas1btr was subsequently purified using the amylose resin column method to recover larger amounts of the protein. The presence of the MBP-Oas1 proteins was confirmed by Western blotting (**Fig. 3**); the proteins were detected using

anti-MBP-HRP antibody. The results of these experiments confirmed the expression and purification of MBP-Oas1 proteins using the pMAL system.

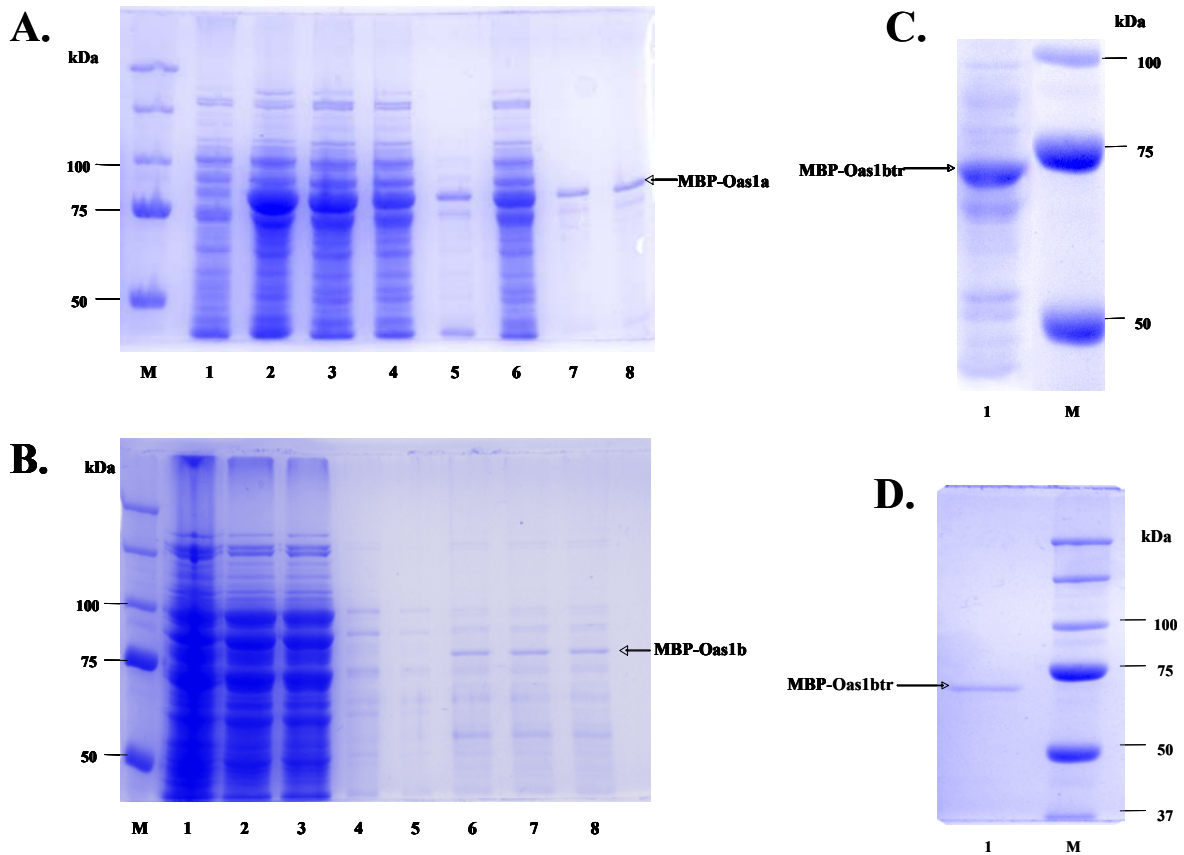


Figure 2: Purification of Oas1 proteins. **(A)** Purification of MBP-Oas1a from BL21 (non-DE3) cells by amylose resin. **Lane 1:** Uninduced cells. **Lane 2:** Cells induced with 1mM IPTG for 18 hrs at 16°C. **Lane 3:** Cell supernatant obtained after French press lysis and centrifugation. **Lane 4:** Flow through #1. **Lane 5:** Wash #1. **Lane 6:** Flow through #2. **Lanes 7 & 8:** Eluate. **(B)** Purification of MBP-Oas1b from BL21 (non-DE3) cells by amylose resin. **Lane 1:** Uninduced cells. **Lane 2:** Cells induced with 1mM IPTG for 18 hrs at 16°C. **Lane 3:** Cell supernatant after French press lysis and centrifugation. **Lane 4:** Flow through. **Lane 5:** Wash. **Lane 6-8:** Eluate. **(C)**

Purification of MBP-Oas1btr with amylose resin. **Lane 1:** Eluate. Proteins were fractionated by 10% SDS-PAGE. **(D)** Purification of MBP-Oas1btr by Ion Exchange Chromatography. **Lane 1:** Eluate. **M:** Molecular weight marker, Precision Plus protein standards (Bio-Rad).

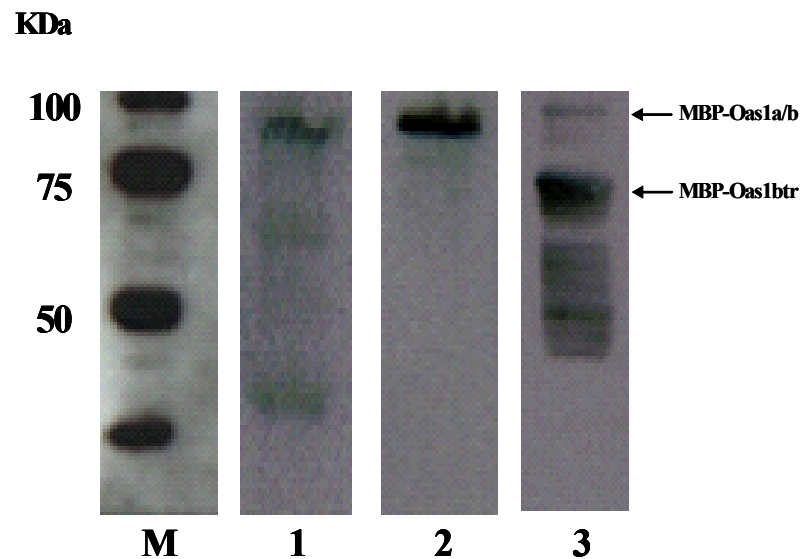


Figure 3: Representative western of MBP-Oas1 proteins purified by amylose resin. **Lane 1:** MBP-Oas1b. **Lane 2:** MBP-Oas1a. **Lane 3:** MBP-Oas1btr. Proteins were separated by 10 % SDS-PAGE. **M:** Molecular weight markers, Precision Plus protein standards (Bio-Rad).

Cleavage of MBP from the MBP-Oas1a fusion protein

Since the MBP-Oas1a fusion protein was the most abundant of the purified proteins, it was used first to see if the MBP fusion could be removed by Genenase I digestion and if Oas1a could successfully be recovered. Digestion with Genenase I was fairly efficient, as there was only a small amount of the fusion protein which could be visualized by gel staining compared to the uncut fusion after 28 hours of digestion (Fig 4, lane 6).

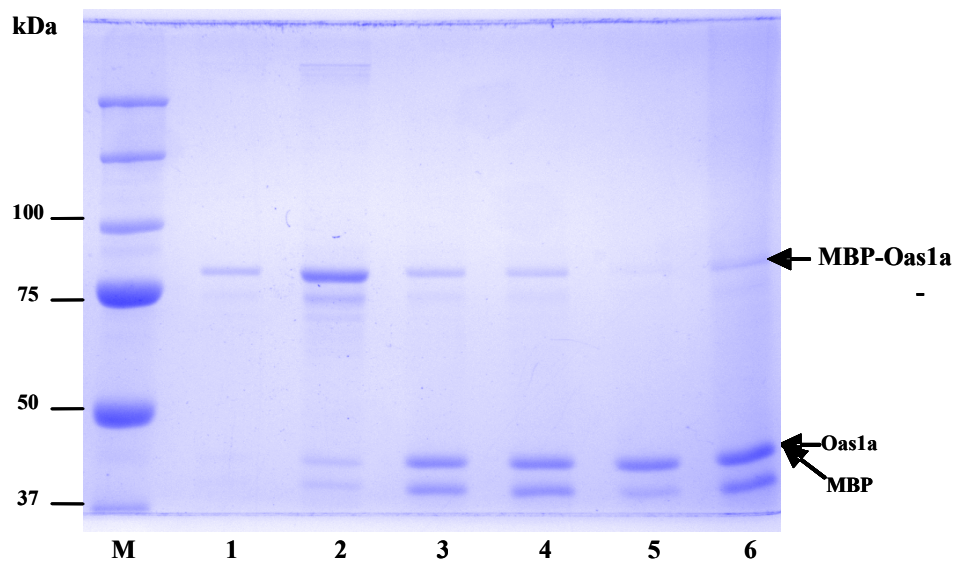


Figure 4: Cleavage of Oas1a from MBP by Genenase I. Approximately 315 μg of purified MBP-Oas1a were digested with Genenase I for 28 hours at room temperature. **Lane 1:** 2 μl of a mock digestion containing protein only was incubated for 28 hrs **Lane 2:** 10 μl of uncut fusion protein **Lane 3:** 10 μl of protein digested for 2 hrs **Lane 4:** 10 μl of protein digested for 4 hrs **Lane 5:** 10 μl of protein digested for 24 hrs **Lane 6:** 10 μl of protein digested for 28 hrs **M:** Molecular weight markers, Precision Plus protein standards (Bio-Rad). Proteins were separated by 10% SDS-PAGE.

After digestion with Genenase I for 28 hrs, undigested MBP fusion protein was separated from released Oas1a using hydroxyapatite and amylose resin chromatography (**Fig. 5A**). Oas1a, the MBP fusion, and Genenase I were eluted from the column; co-elution of Genenase I did not cause a problem since it was present, at most, as 1 % of the eluted proteins. The eluted proteins were then loaded onto an amylose column to bind both free MBP and uncut fusion proteins. However, a limitation of this technique is that any MBP that has been denatured, damaged, or misfolded will not bind to the amylose column and, so will not be removed from the flow-through. Indeed, MBP fusion, which is 42.7 kDa, was detected comigrating with the purified Oas1a, which is 42.5 kDa; this was demonstrated by comparing western blots done with anti-MBP-HRP antibody and anti-OAS1 antibody. Although the SDS-PAGE showed a single band at ~43 kDa, this same band was detected by both antibodies (**Fig. 5B, lanes 3-4**), indicating that some MBP was still present in the purified Oas1a sample. Commercially available MBP2* (42.5 kDa) was not detected with the anti-OAS1 antibody.

The results of these experiments show that although cleavage of MBP from Oas1a was successful, it was not possible to separate the two cleavage products efficiently. Although it may have been possible to separate these two proteins by different methods, such as ion exchange chromatography, other methods were not employed due to the poor recovery of the proteins. In order to investigate whether the removal of the MBP fusion was necessary for synthetase activity, the 2'-5' OAS activity of MBP-Oas1a was next tested.

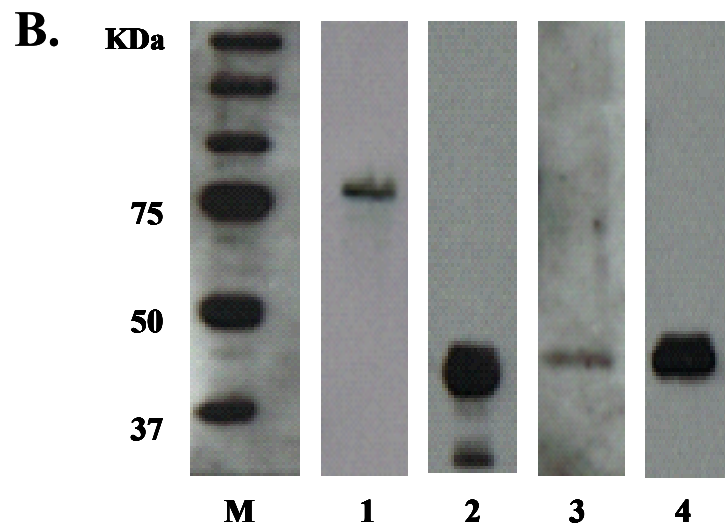
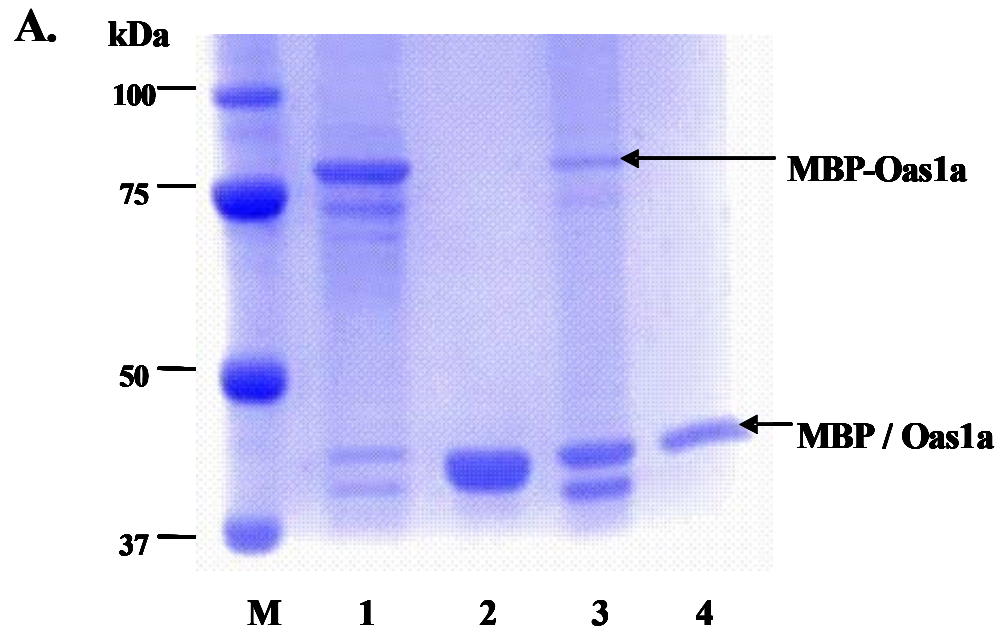


Figure 5: Analysis of cleavage products by western blotting. **(A)** Proteins from a 28 hrs Genenase I cleavage reaction were separated by 10% SDS-PAGE. **Lane 1:** MBP-Oas1a. **Lane 2:** Control MBP2*. **Lane 3:** MBP-Oas1a digested for 24 hrs. **Lane 4:** Oas1a separated by hydroxyapatite chromatography. **(B)** Representative western blots **Lane 1:** Uncut MBP-Oas1a detected with anti-MBP-HRP antibody. **Lane 2:** Control MBP2*

detected with anti-MBP-HRP antibody. **Lane 3:** Hydroxyapatite-purified cleavage products detected with anti-OAS1 antibody. **Lane 4:** Hydroxyapatite-purified cleavage products detected with anti-MBP-HRP antibodies. **M:** Molecular weight marker, Precision Plus protein standards (Bio-Rad). Hydroxyapatite-purified cleavage products were separated by 10% SDS-PAGE.

MBP-Oas1a is a functional synthetase

Based on the crystal structure of the porcine OAS1 protein, Hartmann et al. (2003) predicted that the N-terminal hook of the porcine OAS1 would fold into the protein and pack against the C-terminal domain to form a tether that would maintain a fold which would allow the domain-domain interactions required for enzymatic activity. This structure predicts that the presence of a fusion at the N-terminus of this protein would prevent proper folding and abolish synthetase activity. However, human OAS1 shares greater homology with the porcine OAS1 than do the murine Oas1a or Oas1b proteins. Therefore, it was necessary to test whether an N-terminal fusion would interfere with the enzymatic activity of murine Oas1a. Reaction mixtures containing 2'-5' OAS buffer and different amounts of protein were incubated for 18 hrs at 30°C. The products were separated by 20 % PAGE and the bands visualized by autoradiography.

Previously Kakuta et al. (2002) used bacterially expressed, unpurified Oas1a that contained a 10X histidine tag at its N-terminus to demonstrate that recombinant Oas1a was a functionally active synthetase. MBP-Oas1a showed 2'-5' OAS activity at concentrations from 0.5 µg to 16 µg (**Fig. 6, lanes 4-7**). Purified Oas1a protein, which had the MBP fusion removed, also showed 2'-5' OAS activity (**Fig. 6, lane 3**).

Comparison of the 2-5A synthesized by 0.75 μg of Oas1a and MBP-Oas1a showed that the activities of the two proteins were similar. The lowest tested protein concentration showing detectable synthetase activity was 0.75 μg for Oas1a and 0.5 μg MBP-Oas1a. At concentrations lower than 0.5 μg no activity was detected (data not shown). MBP2*, a commercially available maltose-binding protein, has the same amino acid sequence as the MBP fusion except that it does not contain the 10 amino acid polylinker present in the fusion protein. As a control, MBP2* was also tested for 2'-5' OAS activity (**Fig. 6, lane 2**). MBP2* did not exhibit any 2'-5' OAS activity indicating that the 2'-5' OAS activity shown by the fusion protein could not have been contributed by the MBP fusion. As stated above, since free MBP was not completely removed from Oas1a after cleavage with Genenase I, the Oas1a protein concentration measured was not accurate.

These results showed that bacterially expressed MBP-Oas1a and its cleaved product, Oas1a, were enzymatically functional proteins. Such an observation suggests that the proper folding of MBP-Oas1a into a catalytically active form was not hindered by the presence of the MBP fusion. These results also indirectly confirmed that the MBP-Oas1a protein was able to bind poly (I:C), since binding of poly (I:C) is required to activate a 2'-5' oligoadenylate synthetase.

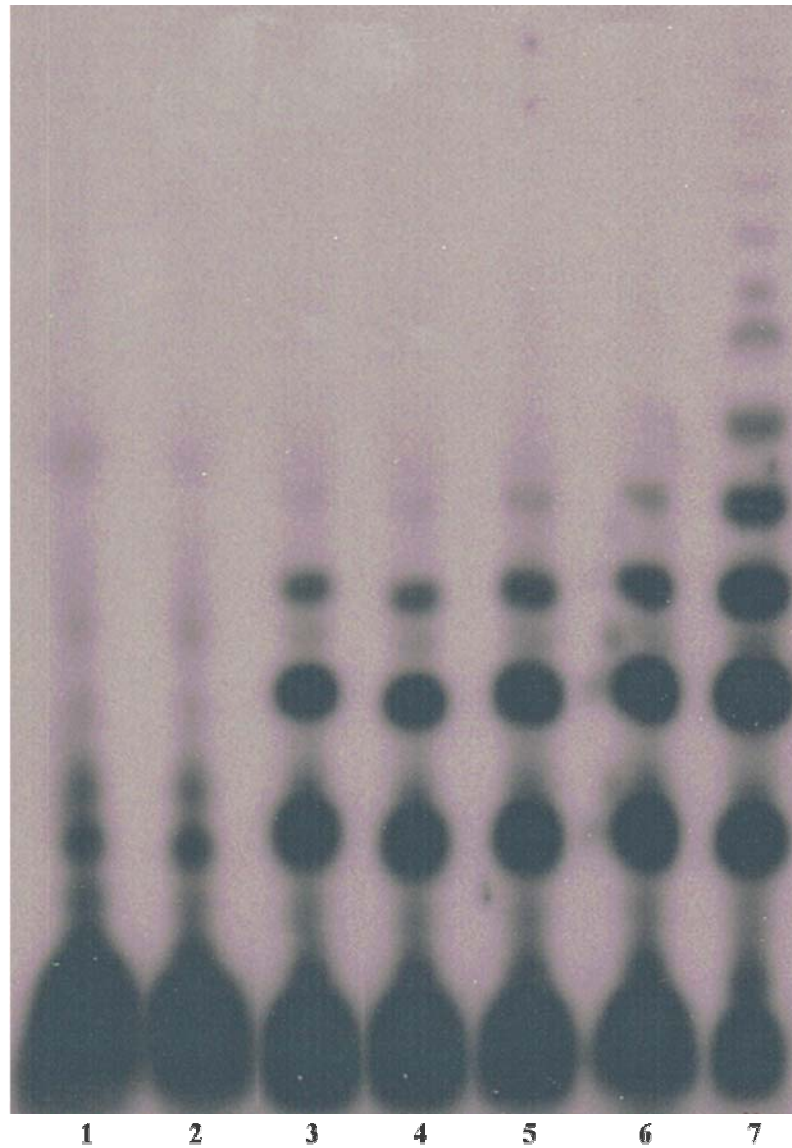


Figure 6: Analysis of the 2-5A synthetase activity of MBP-Oas1a. Different amounts of MBP-Oas1a protein were incubated with $\alpha^{32}\text{p}$ -ATP and poly (I:C) for 18 hrs at 30°C. Four μl of each reaction were separated on a 20% polyacrylamide-urea denaturing gel. **Lane 1:** No protein. **Lane 2:** 16 μg of MBP2*. **Lane 3:** 0.75 μg of Oas1a. **Lane 4:** 0.5 μg of MBP-Oas1a. **Lane 5:** 0.75 μg of MBP-Oas1a. **Lane 6:** 1 μg of MBP-Oas1a. **Lane 7:** 16 μg of MBP-Oas1a.

MBP-Oas1b is a non-functional oligoadenylate synthetase

A truncated form of Oas1b (Oas1btr) was previously cloned from the flavivirus-susceptible C57BL/6J mouse strain, and expressed as an N-terminally 10X histidine-tagged fusion protein in *E. coli*. When this Oas1btr was tested for 2-5A synthetase activity, it was found to be enzymatically non-functional (Kakuta et al., 2002). In the present study, both Oas1a and MBP-Oas1a were shown to have 2'-5' OAS activity (**Fig. 6, lane 3 and lanes 4-7, respectively**); MBP-Oas1a was used as a positive control while MBP-Oas1btr was used as a negative control. The full-length Oas1b, MBP-Oas1b, was tested for synthetase activity. Reaction mixtures containing 2-5A synthetase buffer and different amounts of protein were incubated for 18 hrs at 30°C. The products were separated by 20 % PAGE and the bands visualized by autoradiography. Neither MBP-Oas1b nor MBP-Oas1btr showed any 2'-5' OAS activity (**Fig. 7, lane 3 and lane 2, respectively**) using 2.6 µg of each protein. This concentration was more than 4 times higher than the lowest active concentration of MBP-Oas1a tested. These results demonstrate that MBP-Oas1b is not a functional 2-5A synthetase. However, preliminary results suggest that MBP-Oas1b is able to bind ATP and modify it somehow.

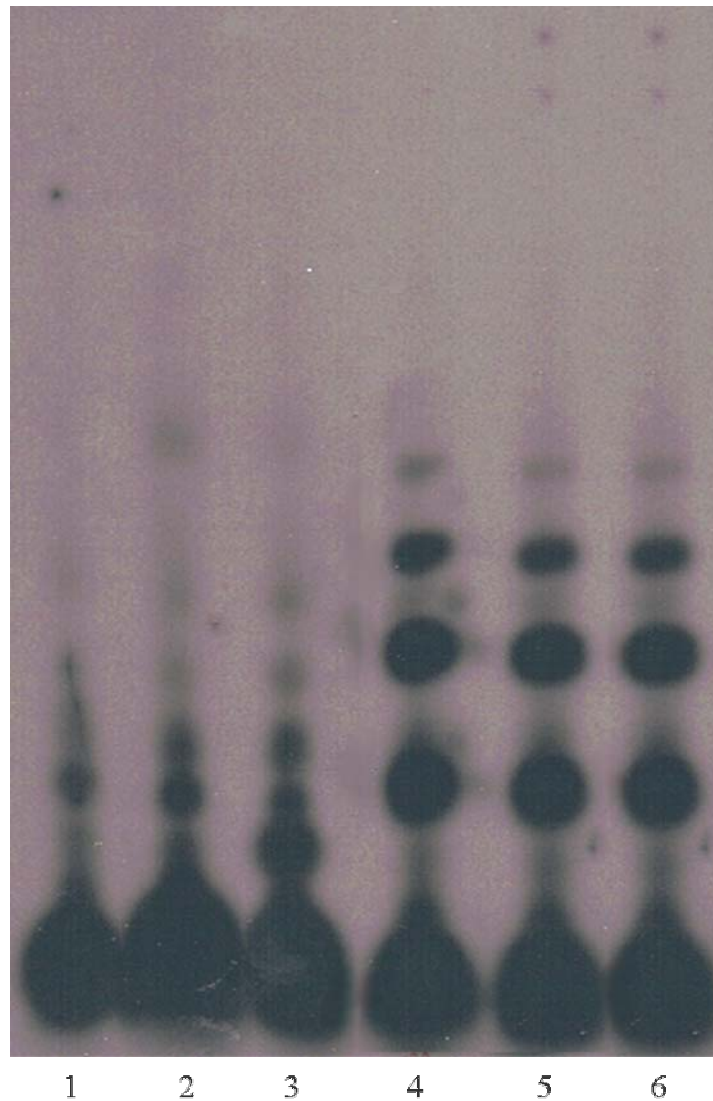


Figure 7: Analysis of the 2'-5' OAS activity of MBP-Oas1b protein. Different amounts of protein were incubated with $\alpha^{32}\text{p}$ -ATP and poly (I:C). Two μl of each reaction were separated on a 20% polyacrylamide-urea denaturing gel. **Lane 1:** No protein. **Lane 2:** 2.3 μg of MBP-Oas1btr. **Lane 3:** 2.6 μg of MBP-Oas1b. **Lane 4:** 1 μg of MBP-Oas1a. **Lane 5:** 0.75 μg of MBP-Oas1a. **Lane 6:** 0.5 μg of MBP-Oas1a.

WNV (+) 3' RNA binding activity of MBP-Oas1 proteins

Activation of 2'-5' Oas proteins requires the binding of dsRNA or some ds-regions within ssRNA. Extensive base pairing is found in several small viral RNA genomes (Maitra et al., 1998; Desai et al., 1995; Sharp et al., 1999). To further investigate the RNA binding activity of MBP-Oas1a, MBP-Oas1b, and MBP-Oas1btr, 3 radiolabeled RNA probes were constructed from different regions of the 3' end of WNV Eg101. The probes were folded using the *mfold* server (Zucher, 2003; Mathews et al., 1999) (**Fig. 8A**) to check that they folded into the optimal secondary structure predicted in a whole genome fold (Sgro and Palmenberg, unpublished data)(**Fig. 8B**).

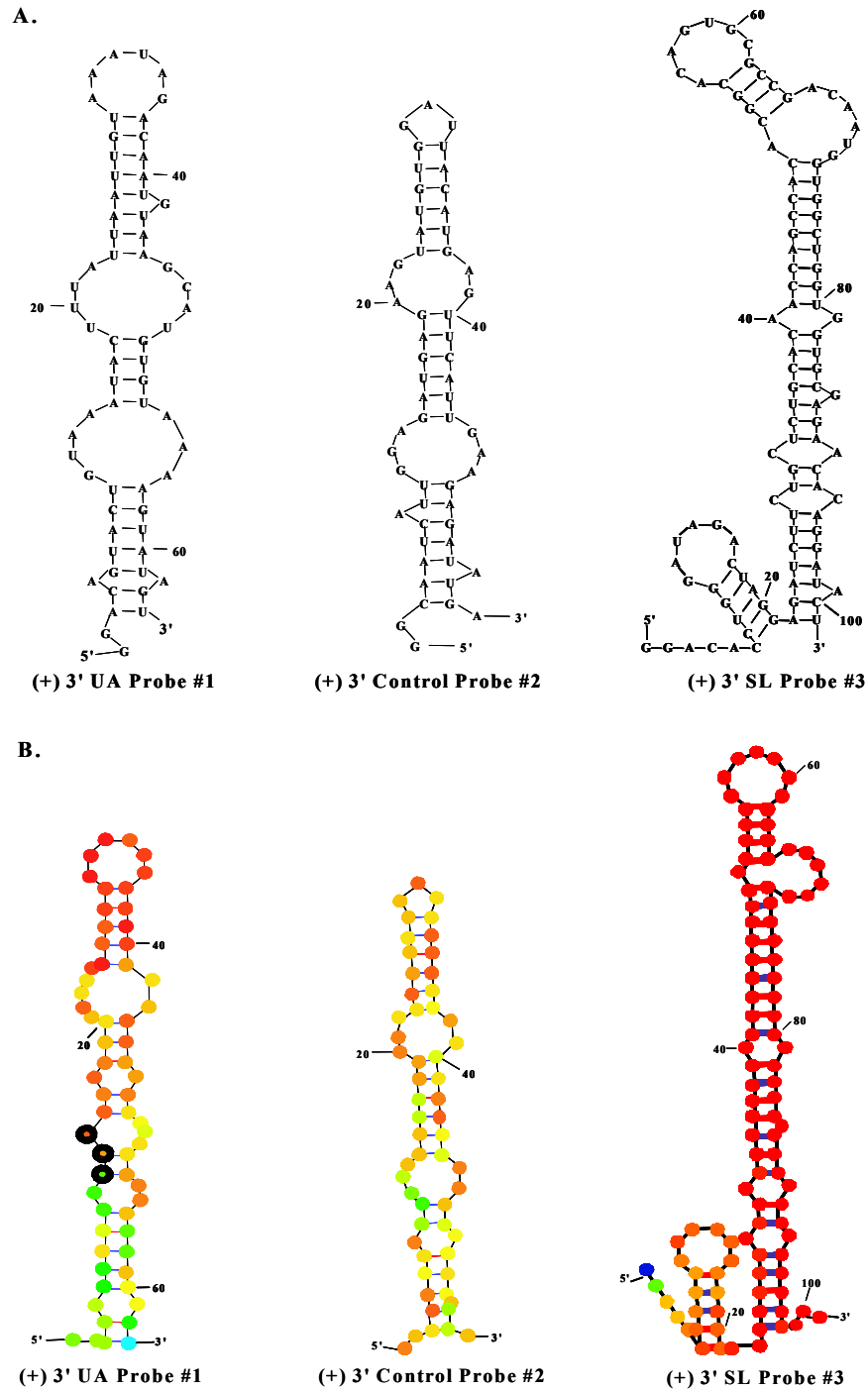


Figure 8: Secondary structure predictions of three WNV RNA probes using only the stem-loop sequence (A) mfold Server (Zucher, 2003; Mathews et al., 1999) or (B) as part of a whole genome fold (Sgro and Palmenberg, unpublished data).

The first probe tested was (+) 3' UA Probe #1, which encompassed nucleotides 10387-10448 of the WNV Eg101 genome. The sequence of this probe spans the last 10 nucleotides of the NS5 viral gene including the stop codon and the first 57 nucleotides of the 3' UTR. This probe has a sequence that is AU-rich. To determine the optimal concentration of non-specific competitor that should be included in RNA binding reactions, MBP2* in large excess (16 μ g) was incubated with (+) 3' UA Probe #1 in the presence of increasing concentrations of yeast tRNA (**Fig. 9**). The data indicated that ~100 ng of tRNA would be sufficient to compete out most of the non-specific binding to MBP2* when it is present in large excess (4 to 16 times) compared to the concentrations used in subsequent gel mobility shift assays. The majority of the non-specific binding activity was competed by the addition of as little as 10 ng of yeast tRNA.

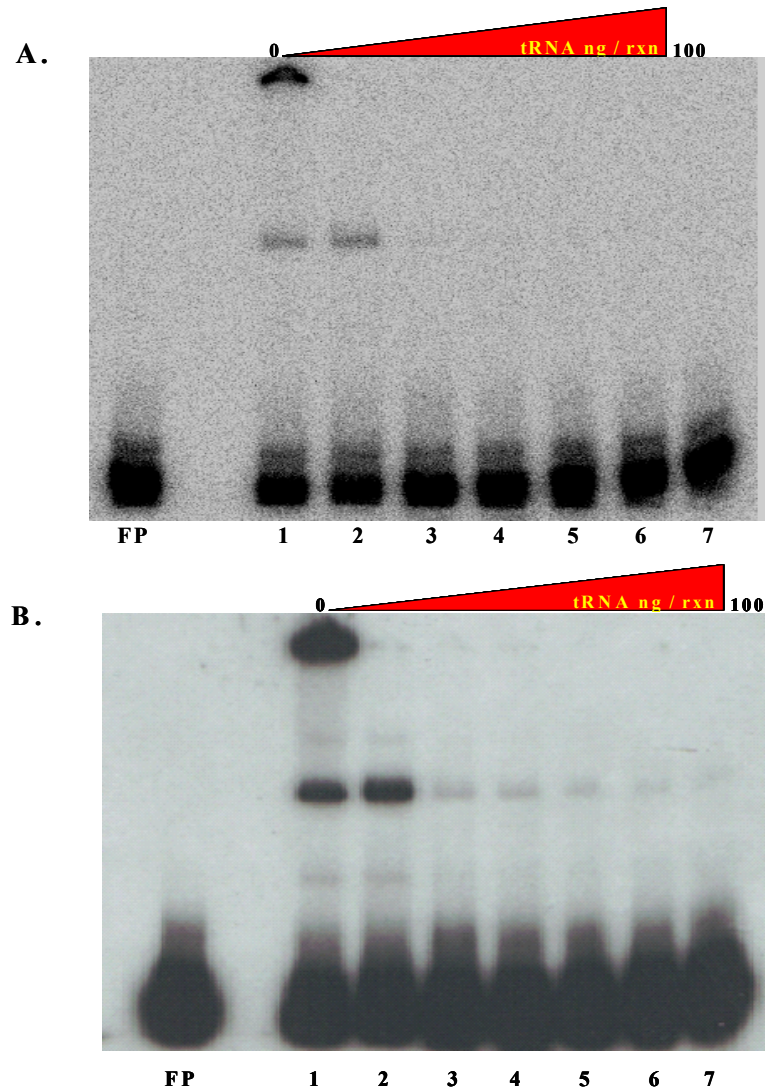


Figure 9: Gel mobility shift assay to determine the optimal non-specific competitor concentration. MBP2* (16 μ g) was incubated with (+) 3' UA Probe #1 (2000 cpm) and increasing concentrations of tRNA. The amounts of competitor were: **Lane 1:** 0. **Lane 2:** 5 ng. **Lane 3:** 10 ng. **Lane 4:** 25 ng. **Lane 5:** 50 ng. **Lane 6:** 75 ng. **Lane 7:** 100 ng. **FP:** Free probe. Binding reactions were separated on a 6 % polyacrylamide non-denaturing gel. Bands on the dried gel were detected by **A.** PhosphorImaging. **B.** Autoradiography.

Based on these results, 30-50 ng of yeast tRNA was used to compete out non-specific binding to the MBP-portion of the fusion proteins and free MBP in the samples. A MBP2* reaction that contained 2 times the highest amount of fusion protein used in the assay was included in each subsequent gel shift experiment. Different concentrations of MBP-Oas1a (200 to 800 ng) and MBP-Oas1b (200 to 600 ng) were next used to test their ability to bind to (+) 3' UA Probe #1 (**Fig. 10**).

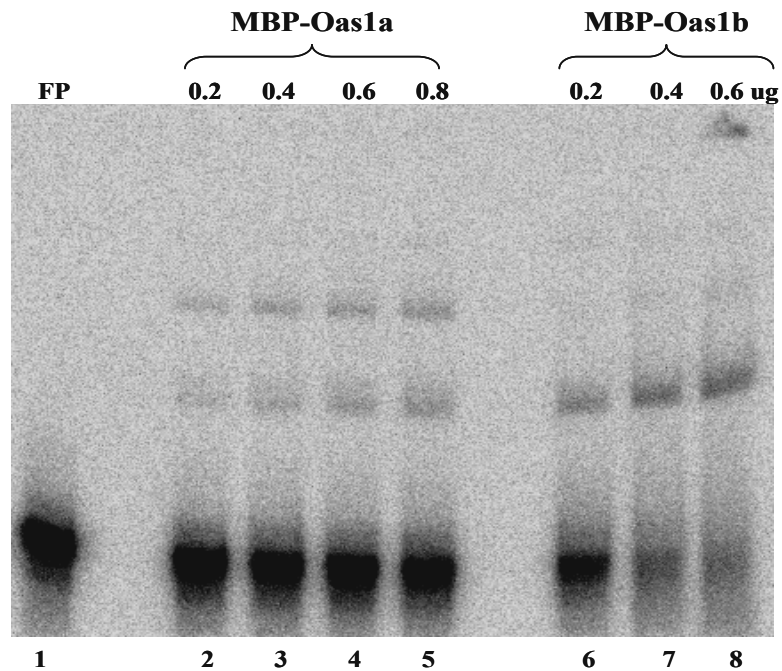


Figure 10: Gel shift mobility assay with (+) 3' UA Probe #1. Various concentrations of MBP-Oas1a (lanes 2-5) or MBP-Oas1b (lanes 6-8) were incubated with (+) 3' UA Probe #1 (2000 cpm). **Lane 1:** Free probe. **Lane 2:** 200 ng of MBP-Oas1a. **Lane 3:** 400 ng of MBP-Oas1a. **Lane 4:** 600 ng of MBP-Oas1a. **Lane 5:** 800 ng of MBP-Oas1a. **Lane 6:** 200 ng of MBP-Oas1b. **Lane 7:** 400 ng of MBP-Oas1b. **Lane 8:** 600 ng of MBP-Oas1b. Binding reactions were separated on a 6 % polyacrylamide non-denaturing gel. Bands on the dried gel were detected by **A.** PhosphorImaging. **B.** Autoradiography.

These results indicated that both MBP-Oas1a and MBP-Oas1b can bind to (+) 3' UA Probe #1; however, the MBP-Oas1b appeared to have a higher binding activity to this probe than MBP-Oas1a. To determine the lowest concentration at which these proteins bind this RNA probe, MBP-Oas1b and MBP-Oas1a at different concentrations below 200 ng were incubated with (+) 3' UA Probe #1. MBP-Oas1b could bind to this RNA probe at concentrations below 10 ng of protein (**Fig. 11**), while RNA binding activity was not detected at 10 ng with MBP-Oas1a (**Fig. 12**). MBP-Oas1btr at concentrations of 10 to 100 ng did not exhibit any binding to (+) 3' UA Probe #1 (**Fig. 13**). MBP2* did not exhibit any binding activity at concentrations twice that of the highest tested concentrations of MBP-Oas1a and MBP-Oas1b, suggesting that the binding of the two Oas1 fusion proteins to (+) 3' Probe #1, was specific.

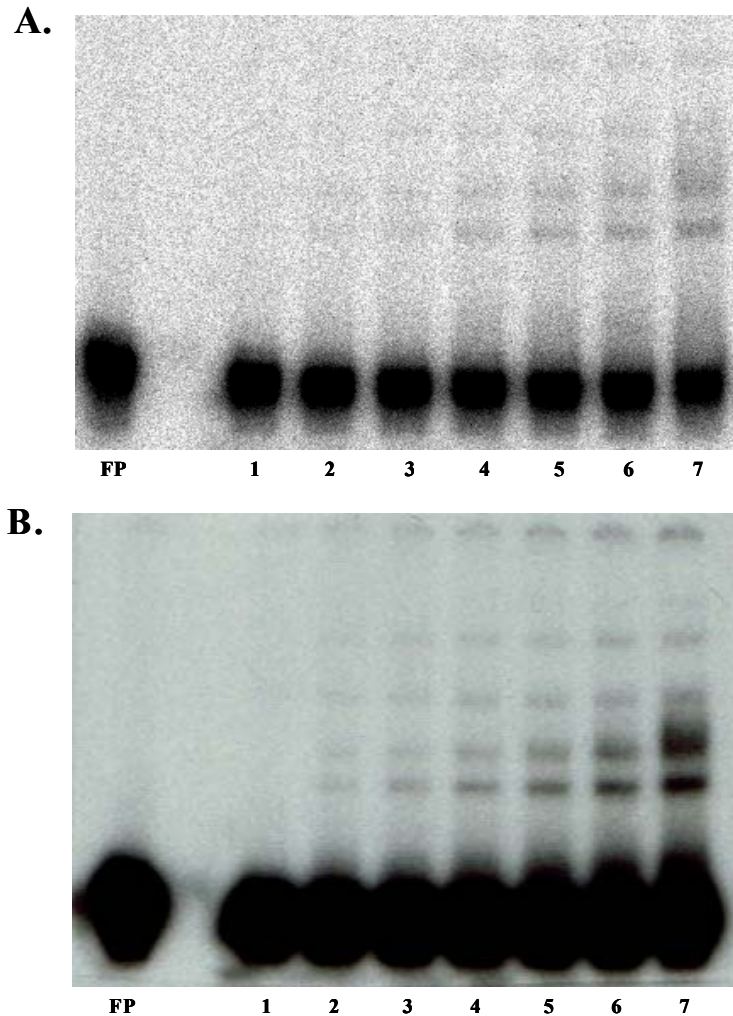


Figure 11: Effect of MBP-Oas1b concentration on binding activity to (+) 3' UA Probe #1. Binding was tested using increasing concentrations of MBP-Oas1b and 2000 cpm of (+) 3' UA Probe #1. **Lane 1:** 200 ng of control MBP2*. **Lane 2:** 10 ng of MBP-Oas1b. **Lane 3:** 25 ng of MBP-Oas1b. **Lane 4:** 50 ng of MBP-Oas1b. **Lane 5:** 75 ng of MBP-Oas1b. **Lane 6:** 100 ng of MBP-Oas1b. **Lane 7:** 200 ng of MBP-Oas1b. **FP:** Free probe. Binding reactions were separated on a 6 % polyacrylamide non-denaturing gel. Bands on the dried gel were detected by **A.** PhosphorImaging. **B.** Autoradiography.

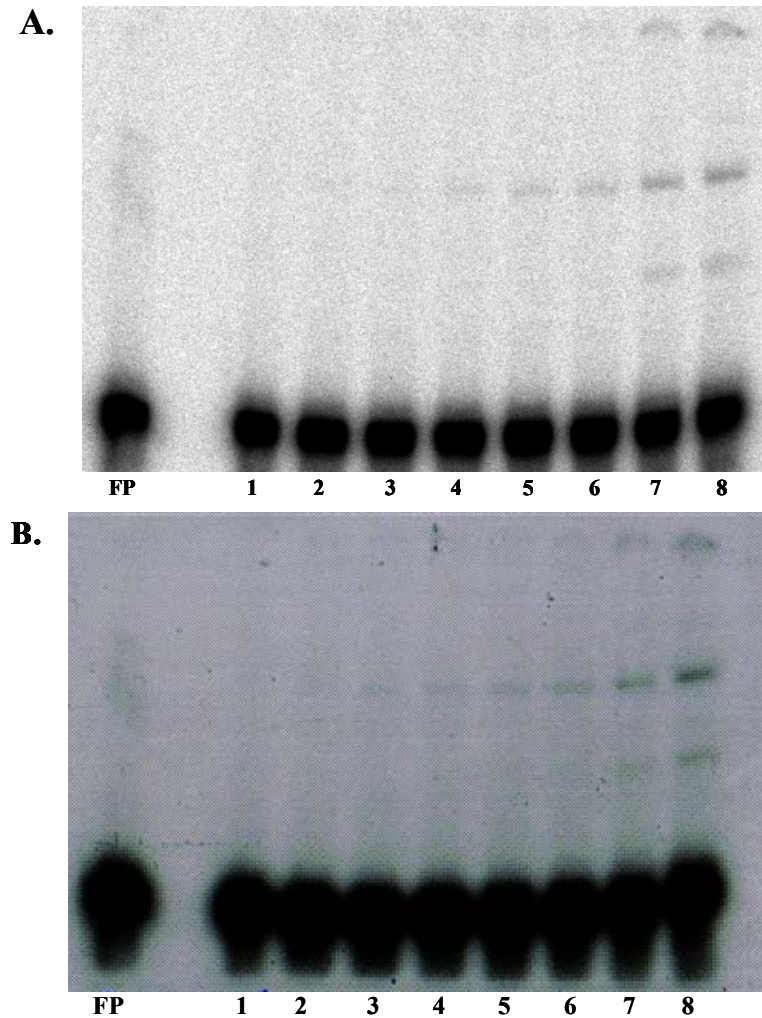


Figure 12: Effect of MBP-Oas1a concentration on binding activity to (+) 3' UA Probe #1. Binding was tested using increasing concentrations of MBP-Oas1a and 2000 cpm of (+) 3' UA Probe #1. **Lane 1:** 400 ng of control MBP2*. **Lane 2:** 10 ng of MBP-Oas1a. **Lane 3:** 25 ng of MBP-Oas1a. **Lane 4:** 50 ng of MBP-Oas1a. **Lane 5:** 75 ng of MBP-Oas1a. **Lane 6:** 100 ng of MBP-Oas1a. **Lane 7:** 200 ng of MBP-Oas1a. **Lane 8:** 400 ng of MBP-Oas1a. **FP:** Free probe. Binding reactions were separated on a 6 % polyacrylamide non-denaturing gel. Bands on the dried gel were detected by **A.** PhosphorImaging. **B.** Autoradiography.

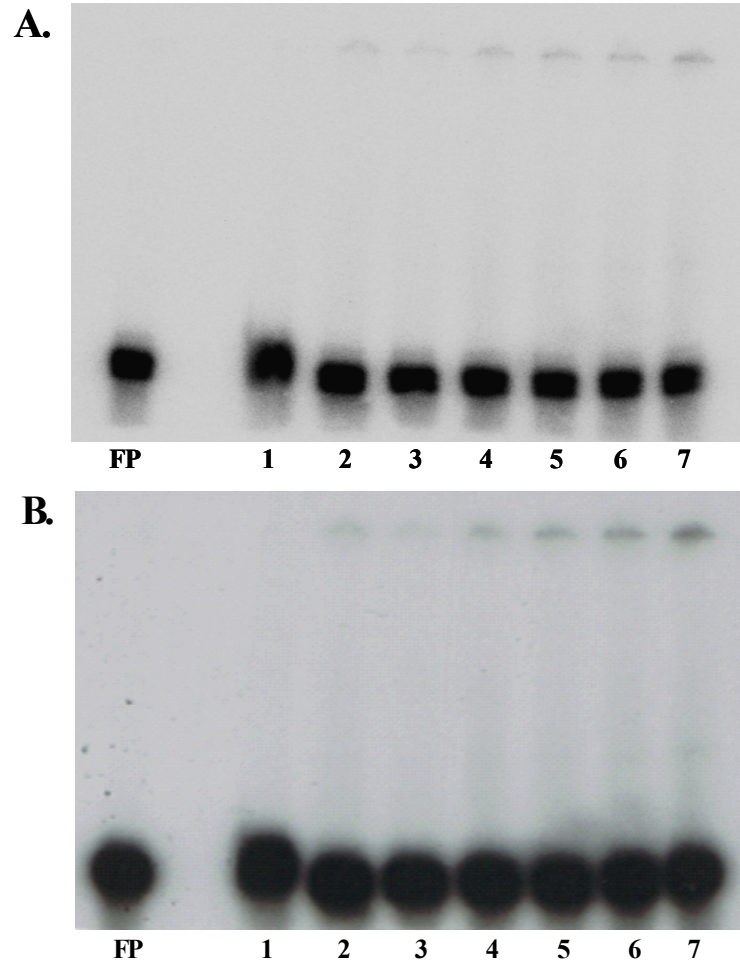


Figure 13: Effect of MBP-Oas1btr concentration on binding activity to (+) 3' UA Probe #1. Binding was tested using increasing concentrations of MBP-Oas1btr and 2000 cpm of (+) 3' UA Probe #1. **Lane 1:** 200 ng of control MBP2*. **Lane 2:** 10 ng of MBP-Oas1btr. **Lane 3:** 25 ng of MBP-Oas1btr. **Lane 4:** 50 ng of MBP-Oas1btr. **Lane 5:** 75 ng of MBP-Oas1btr. **Lane 6:** 100 ng of MBP-Oas1btr. **Lane 7:** 200 ng of MBP-Oas1btr. **FP:** Free probe. Binding reactions were separated on a 6 % polyacrylamide non-denaturing gel. Bands on the dried gel were detected by **A.** PhosphorImaging. **B.** Autoradiography.

The next RNA probe tested was the (+) 3' Control Probe #2, which encompasses nucleotides 10308-10364 of the WNV Eg101 genome. The (+) 3' Control Probe #2 is located in the 3' end of the NS5 gene of WNV Eg101 and is also rich in As and Us. Although it has a secondary structure that is similar to (+) 3' UA Probe #1, it does not contain uninterrupted single-stranded stretches of As and Us that are as long as those in (+) 3' UA Probe #1. MBP-Oas1 protein concentrations of 25 ng, 50 ng, and 100 ng were used to test the efficiency of binding of this protein to (+) 3' Control Probe #2 (**Fig. 14, for MBP-Oas1b and MBP-Oas1a; Fig. 15, for MBP-Oas1b and MBP-Oas1btr**). MBP-Oas1b but neither MBP-Oas1a nor MBP-Oas1btr exhibited detectable binding to the (+) 3' Control Probe #2. Notably, the relative binding activity of MBP-Oas1b to this RNA probe was similar to that observed with (+) 3' UA Probe #1. However, competition gel shift assays using these two probes are required to quantify these interactions.

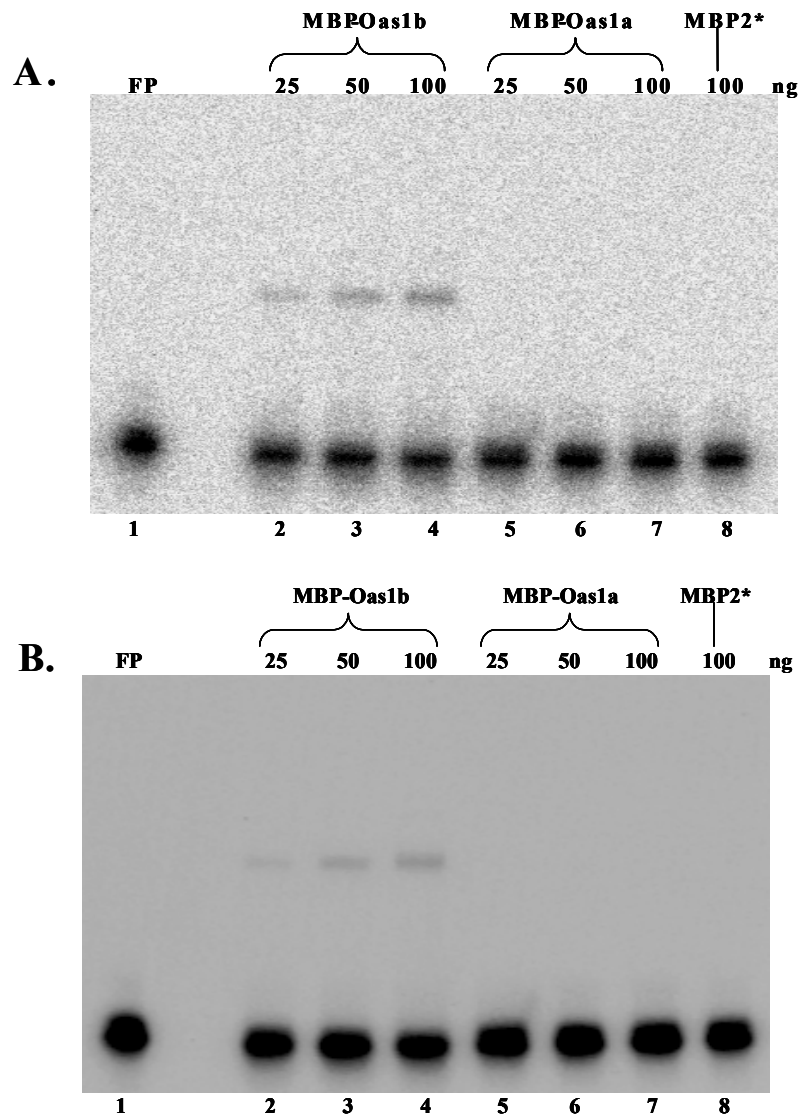


Figure 14: Gel mobility shift assay with (+) 3' Control Probe #2. Increasing concentrations of MBP-Oas1b or MBP-Oas1a were incubated with (+) 3' Control Probe #2 (1000 cpm). **Lane 1:** Free probe. **Lane 2:** 25 ng of MBP-Oas1b. **Lane 3:** 50 ng of MBP-Oas1b. **Lane 4:** 100 ng of MBP-Oas1b. **Lane 5:** 25 ng of MBP-Oas1a. **Lane 6:** 50 ng of MBP-Oas1a. **Lane 7:** 100 ng of MBP-Oas1a. **Lane 8:** 100 ng of control MBP2*. Binding reactions were separated on a 6 % polyacrylamide non-denaturing gel. Bands on the dried gel were detected by **A.** PhosphorImaging. **B.** Autoradiography.

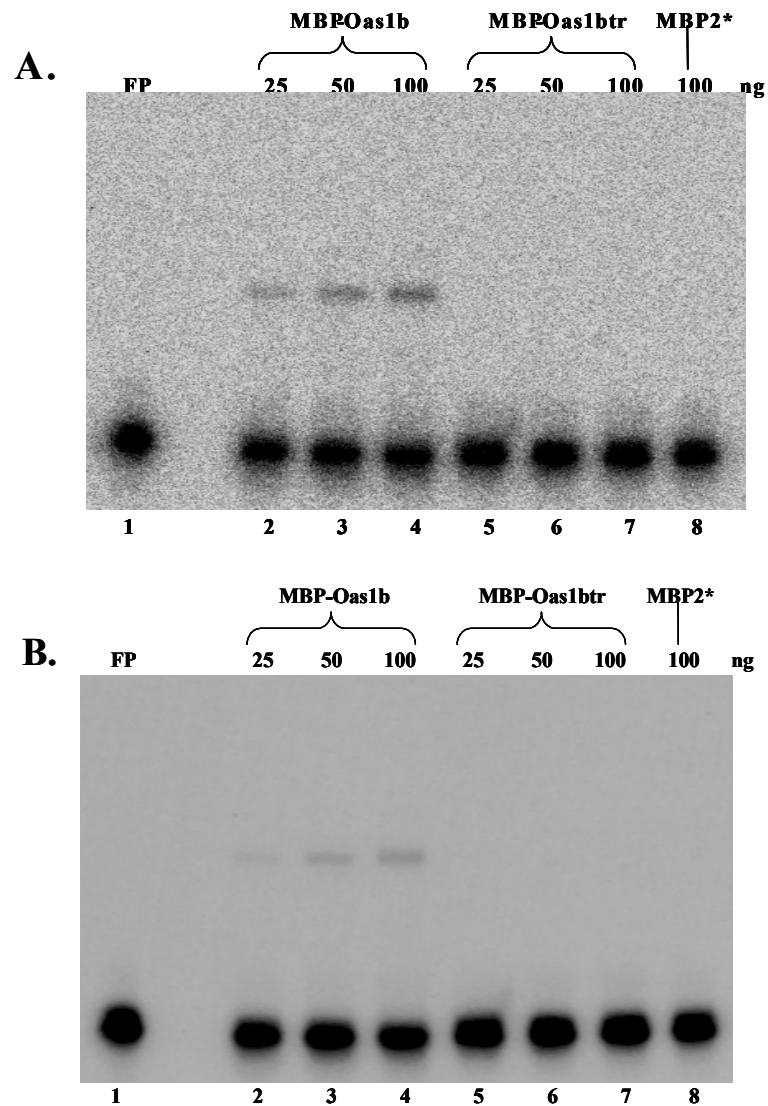


Figure 15: Gel mobility shift assay with (+) 3' Control Probe #2. Increasing concentrations of MBP-Oas1b or MBP-Oas1btr were incubated with (+) 3' Control Probe #2 (1000 cpm). **Lane 1:** Free probe. **Lane 2:** 25 ng of MBP-Oas1b. **Lane 3:** 50 ng of MBP-Oas1b. **Lane 4:** 100 ng of MBP-Oas1b. **Lane 5:** 25 ng of MBP-Oas1btr. **Lane 6:** 50 ng of MBP-Oas1btr. **Lane 7:** 100 ng of MBP-Oas1btr. **Lane 8:** 100 ng of control MBP2*. Binding reactions were separated on a 6 % polyacrylamide non-denaturing gel. Bands on the dried gel were detected by **A.** PhosphorImaging. **B.** Autoradiography.

The last probe tested was (+) 3' SL Probe #3, which comprised the 3' terminal stem-loop structure of WNV Eg101. MBP-Oas1 protein at concentrations of 25 ng, 50 ng, and 100 ng were used to test the binding activity of this protein to (+) 3' SL Probe #3 (**Fig. 16, for MBP-Oas1b and MBP-Oas1btr; Fig. 17, for MBP-Oas1b and MBP-Oas1a**). Interestingly, this probe did not bind to any of the Oas1 fusion proteins. This is the longest of the probes used and it contains the longest stretches of dsRNA.

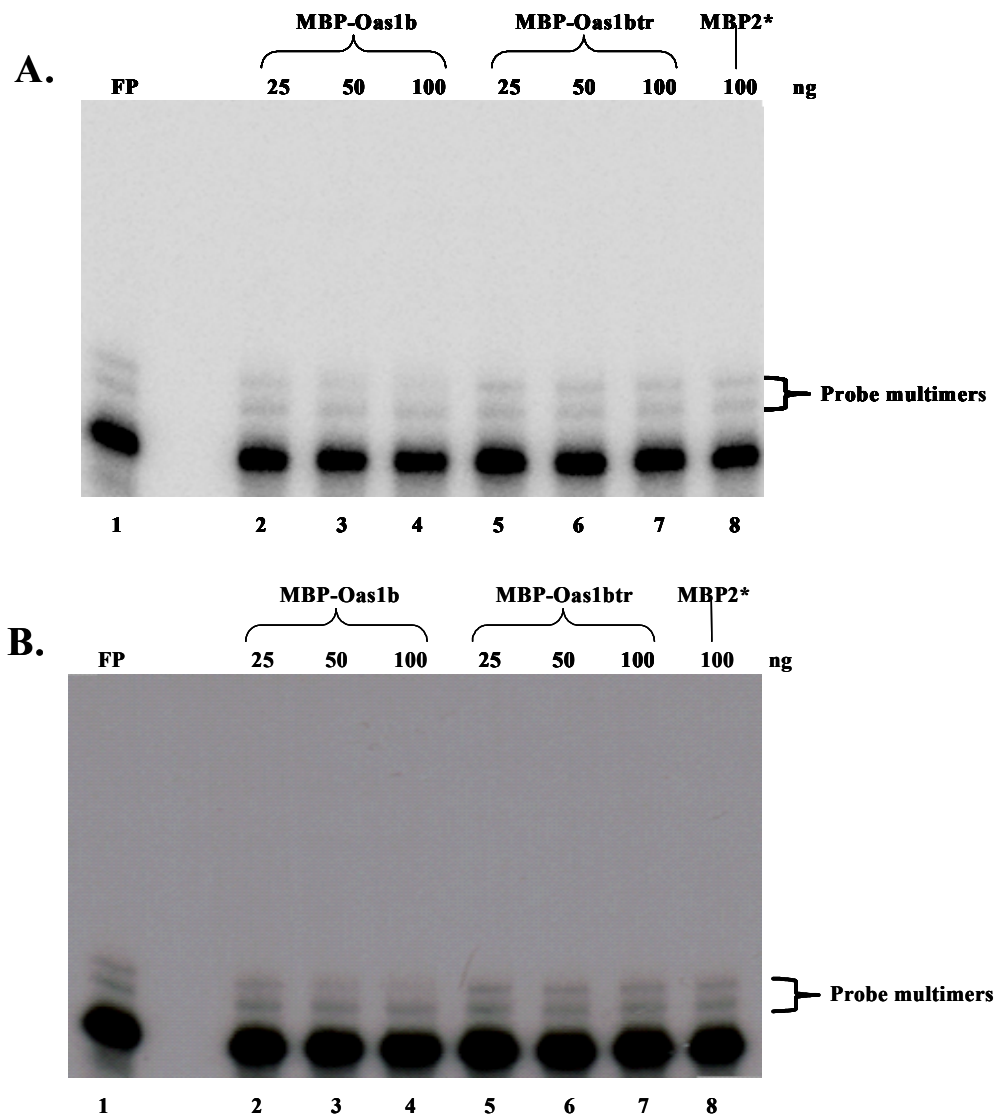


Figure 16: Gel mobility shift assay with (+) 3' SL Probe #3. Increasing concentrations of MBP-Oas1b or MBP-Oas1btr were incubated with (+) 3' SL Probe #3 (1000 cpm). **Lane 1:** Free probe. **Lane 2:** 25 ng of MBP-Oas1b. **Lane 3:** 50 ng of MBP-Oas1b. **Lane 4:** 100 ng of MBP-Oas1b. **Lane 5:** 25 ng of MBP-Oas1btr. **Lane 6:** 50 ng of MBP-Oas1btr. **Lane 7:** 100 ng of MBP-Oas1btr. **Lane 8:** 100 ng of control MBP2*. Binding reactions were separated on a 6 % polyacrylamide non-denaturing gel. Bands on the dried gel were detected by **A.** PhosphorImaging. **B.** Autoradiography.

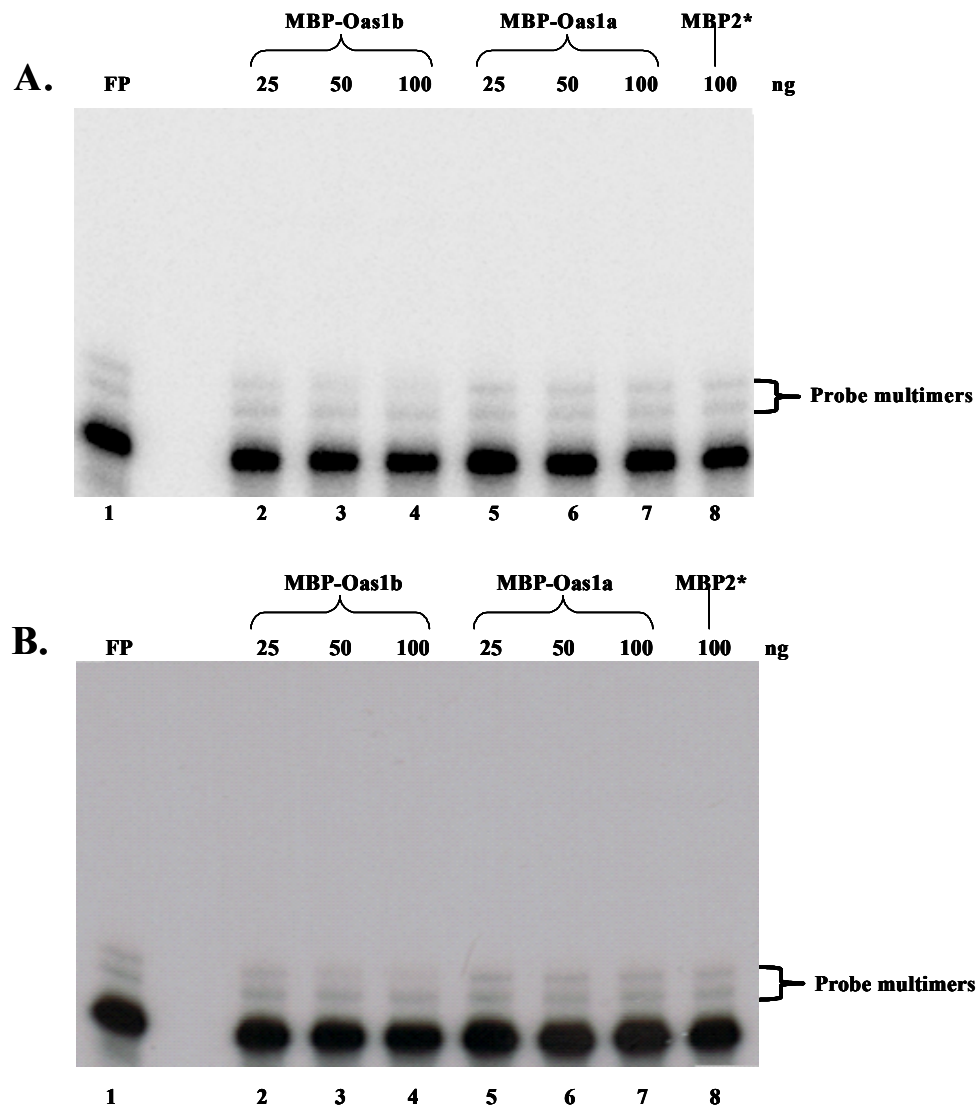


Figure 17: Gel mobility shift assay with (+) 3' SL Probe #3. Increasing concentrations of MBP-Oas1b or MBP-Oas1a were incubated with (+) 3' SL Probe #3 (1000 cpm). **Lane 1:** Free probe. **Lane 2:** 25 ng of MBP-Oas1b. **Lane 3:** 50 ng of MBP-Oas1b. **Lane 4:** 100 ng of MBP-Oas1b. **Lane 5:** 25 ng of MBP-Oas1a. **Lane 6:** 50 ng of MBP-Oas1a. **Lane 7:** 100 ng of MBP-Oas1a. **Lane 8:** 100 ng of control MBP2*. Binding reactions were separated on a 6 % polyacrylamide non-denaturing gel. Bands on the dried gel were detected by **A.** PhosphorImaging. **B.** Autoradiography.

MBP-Oas1b but not MBP-Oas1btr inhibits MBP-Oas1a synthetase activity in vitro

Addition of Oas1d, a non-functional synthetase, to Oas1a in 2-5A synthetase reactions was recently reported to have an inhibitory effect on the synthetase activity of Oas1a (Yan et al., 2005). To investigate whether the non-functional MBP-Oas1b or MBP-Oas1btr could inhibit the synthetase activity of MBP-Oas1a *in vitro*, 2-5A synthetase reactions containing 1 μ g of MBP-Oas1a and increasing amounts of either MBP-Oas1b or MBP-Oas1btr (0, 0.5X, 1X, 1.5X, and 2X) were analyzed. The results showed that MBP-Oas1b inhibited MBP-Oas1a synthetase activity in a dose-dependant manner (**Fig. 18, lanes 2-6**). However, this inhibitory effect was not observed after the addition of MBP-Oas1btr (**Fig. 18, lanes 7-10**). Both ATP and poly (I:C) were in excess in these reactions.

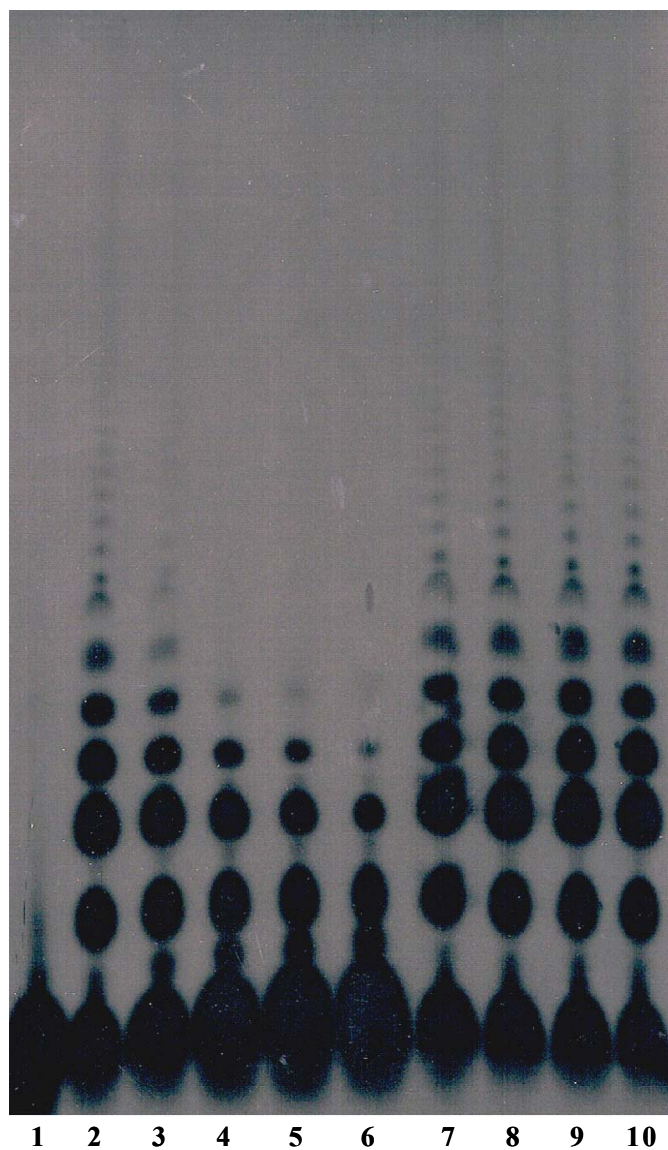


Figure 18: Inhibition of MBP-Oas1a synthetase activity. All reactions contained $\alpha^{32}\text{p}$ -ATP, poly (I:C), and 1 μg of MBP-Oas1a, except **Lane 1**, which contained no proteins. In addition to MBP-Oas1a, reactions also contained: **Lanes 2-6:** 0, 0.5X, 1X, 1.5X, or 2X of MBP-Oas1b, respectively. **Lanes 7-10:** 0, 0.5X, 1X, 1.5X, or 2X of MBP-Oas1btr, respectively. Four μl of each reaction were separated on a 20% polyacrylamide-urea denaturing gel.

DISCUSSION

Expression and Purification of murine Oas1 proteins

Kakuta et al. (2002), expressed Oas1btr using the pET expression system in a previous study. The expressed Oas1btr protein was not purified; instead crude cell extracts were used in their studies of Oas1 synthetase activity and poly (I:C) binding. In the present study, efficient and soluble expression of murine Oas1b was not achieved using the pET system. To investigate whether poor expression levels were a characteristic of the Oas1b protein, Oas1btr was next expressed using the pET expression system. Expression levels of Oas1btr were not significantly greater than of Oas1b; the solubility of Oas1btr was not determined. Expression of Oas1a was not attempted using this system. It is not clear why the levels of soluble Oas1b/btr were so low when expressed using this system. Oas1a shares 82% amino acid sequence homology with Oas1b, with the greatest variability in the C-terminus and the next greatest variability in the N-terminus. The two proteins are most homologous within the central, nucleotidyltransferase domain. Hydrophobicity plots of the amino acid sequences of both Oas1a and Oas1b showed that the tail of the Oas1b protein is more hydrophobic than that of Oas1a. The hydrophobic sequence at the C-terminus of Oas1b may have contributed to the expression of insoluble protein using the pET expression system.

Subsequently, the pMAL Protein Fusion and Purification System was used to express Oas1a, Oas1b and Oas1btr as MBP-fusion proteins in bacteria. All 3 of the Oas1 proteins expressed using the pMAL system were soluble and expressed at levels adequate for purification. However, the observed expression level of MBP-Oas1a was significantly higher than that of either MBP-Oas1btr or MBP-Oas1b. Relative to MBP-

Oas1b, MBP-Oas1btr was expressed at lower levels. The purified proteins were subsequently used in *in vitro* 2-5A synthetase assays and in gel shift mobility assays with RNA probes from the 3' end of the WNV genomic RNA.

2'-5' oligoadenylate synthetase activity

Oas1a and Oas1g were previously reported to be functional 2'-5' oligoadenylate synthetases (Kakuta et al., 2002). In that study, Oas1 proteins in bacterial lysates were incubated with poly (I:C)-agarose bead, the bound proteins were then used in a 2-5A synthetase activity assay. Using this technique, variation in activation of the Oas1 proteins by poly (I:C) could in part be due to differences in the poly (I:C) binding activities of the tested proteins. Bacterial proteins present in the crude cell extracts also may compete with Oas1 proteins for binding of poly (I:C), producing results that may be unreliable. Although Oas1btr was tested by Kakuta et al. (2002) and found not to be active, it was found to bind poly (I:C). Full-length Oas1b was not previously tested for RNA binding or synthetase activity. In the present study, neither MBP-Oas1b nor MBP-Oas1btr showed detectable 2-5A synthetase activity. Under the same conditions, MBP-Oas1a produced 2-5A oligomers.

A previous study showed that enzyme activity was almost completely lost when mutations were introduced in the putative active sites of human OAS isozymes (Sarkar et al., 2002). The Oas1b protein contains R90Q and R91Q substitutions in the substrate binding acceptor site, and also S203R and K209T substitutions in the substrate binding donor site. Oas1b also has a 4 amino acid deletion in the P-loop which may prevent it from folding into a catalytically functional structure. These mutations predicted that the

full-length Oas1b protein would not be an active synthetase. The results in the present study confirmed the prediction that Oas1b is not a functional 2-5A synthetase.

The production of 2-5A and its subsequent activation of RNase L are important components of one of the IFN-induced antiviral pathways in cells. There is a growing amount of evidence that 2-5A synthetases can participate in non-enzymatic cellular functions. For instance, an alternatively spliced product of the human OAS1 gene designated 9-2/E17 is an active synthetase. Interestingly, this isozyme also contains a BH3 domain through which it has been reported to interact with Bcl-2 family proteins inducing apoptosis (Ghosh et al., 2001), demonstrating that this protein has two mutually independent activities, namely, synthesizing 2-5A and promoting apoptosis. A yeast two-hybrid system was used to screen a human B cell cDNA library with PRL-R (prolactin receptor) and a human OAS1 isoform was reported to interact with PRL-R. Overexpression of the human OAS1 decreased the basal activity of both the IRF-1 and β -casein promoters by 40-60 % via an RNase L-independent mechanism (McAveney et al., 2000; Zhou et al., 1993). Overexpression of both PRL and OAS1 decreased IRF-1 promoter activity by 60% (McAveney et al., 2000).

Inhibition of Oas1a synthetase activity

Human OAS1 proteins have a CFK motif at their C-terminus which is required for tetramerization of these proteins (Ghosh et al., 1997). Hartmann et al. (2003) reported that the porcine OAS1, which is 73 % identical in sequence to human OAS1, crystallized as a monomeric protein. Amino acids important for folding of the porcine OAS1 and the mouse Oas1b share an overall identity of 56 % (Hartmann et al., 2003). The ability of

mouse Oas1 proteins to multimerize has not yet been investigated. The CFK motif is conserved in the full-length Oas1b protein, but the Oas1a protein contains a K to I substitution in this motif and it is possible that this mutation could affect protein-protein interactions facilitated via the CFK motif. Yan et al. (2005) demonstrated that Oas1a synthetase activity was inhibited by addition of Oas1d *in vitro*, presumably via direct protein-protein interactions. Once activated by dsRNA, Oas1a is ubiquitously expressed in multiple tissues. The ovary-specific expression pattern of Oas1d, suggests a role for this protein during oogenesis and/or embryogenesis. Oas1c and Oas1e, which are other non-functional synthetases, are also abundantly expressed in oocytes. Upon viral infection, the Oas1a-mediated IFN response is ubiquitous. The authors suggest that this inhibitory effect of Oas1d could serve a protective function by blocking or down-regulating the IFN/OAS/RNase L RNA degradation pathway to prevent the loss of oocytes during acute viral infection; thus maintaining female fertility. However, Oas1d may have an RNase L independent function in regulating development.

In the present study, MBP-Oas1b was shown to inhibit MBP-Oas1a synthetase activity. The resistant phenotype is characterized by a 100-fold or more decrease in the amount of intracellular viral RNA; thus, any inhibition of Oas1a synthetase activity by Oas1b *in vivo* would be inconsistent with the theory that a mechanism involving RNase L mediated viral RNA degradation via 2-5A synthetase activity confers flavivirus resistance. In support of the validity of the interaction between MBP-Oas1a and MBP-Oas1b, the inhibitory effect was not observed after the addition of MBP-Oas1btr (**Fig 18, lanes 7-10**). Oas1btr has a C-terminal truncation that may prevent protein-protein interactions. The results of the present study showed that MBP-Oas1b is not a functional

synthetase and that it can inhibit the 2-5A synthetase activity of Oas1a. These data suggest that Oas1b confers the flavivirus resistance phenotype through a mechanism that is independent of the RNase L-RNA degradation pathway.

RNA binding activity

Poly (I:C) has been used as the standard activator of IFN and OAS for decades (Minks et al., 1979); however, it is a synthetic RNA that is not present in cells. Poly (I:C) consists of double strands formed by homopolymers that are not interrupted by single-stranded bulges or loops. Cellular RNAs are single-stranded but can form secondary and tertiary interactions. Longer synthetic dsRNAs (40 to 110 bp) have been reported to activate 2-5A synthetases more efficiently than shorter dsRNAs (25 bp) at subsaturating concentrations of ~100 nM (Desai and Sen, 1997). Full activation by the short dsRNAs is only observed at saturating concentrations (Sarkar et al., 1999). Han and Barton (2002) reported a threshold concentration of 20 nM of HCV mRNA for activation of human 2-5A synthetase. In comparison to the standard poly (I:C) concentration used for activation of 2-5A synthetases (50 µg/ml), full activation of human 2-5A synthetase activity in HeLa cell extracts by HCV genome RNA (~9.6 kb) required a concentration of ~350 µg/ml. These observations suggest that although a high level of activation of 2-5A synthetases is achieved by relatively low concentrations of poly (I:C), the physiological levels of viral RNAs in infected cells would not be sufficient to achieve significant levels of RNase L activation until late in the infection cycle. The effect of the flavivirus resistance phenotype on viral RNA can be observed as early as 2 hrs after infection (Yan and Brinton, unpublished data).

Kakuta et al. (2002) reported RNA binding activity of Oas1a and Oas1btr using poly (I:C)-agarose beads that were incubated with crude cell lysates prepared from bacterial cultures expressing Oas1 proteins. The bound Oas1 proteins were detected using anti-His antibody. All Oas1 proteins tested in that study exhibited binding to poly (I:C). However, some of the binding activity observed could have been due to other bacterial proteins, similar in size to the Oas1 proteins and with His-rich regions, which may non-specifically bind. The anti-His antibody can detect cell proteins rich in His residues, such as heat-shock proteins. Because poly (I:C)-agarose beads are no longer commercially available and because attempts to make poly (I:C)-agarose beads in the lab failed, poly (I:C)-agarose beads were not used to study Oas1 protein-RNA interactions. However, poly (I:C) was used to activate Oas1 synthetase activity. RNA probes synthesized from the 3' end of WNV Eg101 were used to compare the RNA binding activity of the Oas1 proteins.

Among flaviviruses, the 3' terminal region of the genome RNAs contains conserved structures, despite exhibiting little sequence homology. Many flavivirus genomes contain regions that are rich in As and Us in their 3' UTR immediately following the stop codon. The sequences within these regions may be targets for RNase L digestion which occurs at UA and UU dinucleotides. The 3' terminal stem-loop that is the most highly conserved of the 3' UTR structures among divergent flaviviruses. According to secondary structure predictions based on the whole genome fold, the next two proximal stem-loop structures with relatively high probability of forming are located at the end of the NS5 gene and in the 5' region of the 3' UTR. The RNA binding activities of the various MBP-Oas1 fusion proteins to the three WNV 3' probes was

compared. Both MBP-Oas1a and MBP-Oas1a showed binding to the AU-rich probes located at or near the 5' end of the 3' UTR. Neither MBP-Oas1a nor MBP-Oas1b bound to the 3' stem-loop at the protein concentrations tested. In contrast to the previous results that demonstrated binding of Oas1btr to poly (I:C)-agarose (Kakuta et al., 2002), MBP-Oas1btr did not bind to any of the probes tested. Results presented in this study, demonstrate that MBP-Oas1b and MBP-Oas1a exhibit RNA binding activity to regions of the 3' end of the WNV genomic RNA. To our knowledge this is the first report of specific interactions between a 2'-5' oligoadenylate synthetase and particular regions of a viral genome. These results suggest that if the flavivirus resistance mechanism mediated by Oas1b involves viral RNA-protein interactions and/or protein-protein interactions, then the truncated form of Oas1b expressed in susceptible cells would not be able to mediate these interactions.

Future directions

The 2-5A synthetase activity of three mouse Oas1 proteins was tested in the present study using poly (I:C). MBP-Oas1a was the only functional synthetase. In future studies, the ability of different regions of the WNV RNA to activate Oas1 proteins will be investigated.

Results from the present study suggest that the structures of the human and porcine OAS1 proteins may differ from that of the mouse Oas1 proteins. Crystallization studies and subsequent comparison of the crystal structures of the porcine OAS1 protein and the mouse Oas1a or Oas1b proteins will require the production of large amounts of Oas1 proteins and for this, *in vitro* transcription/translation systems or the

baculovirus/insect expression system will be used. As one means of detecting cellular or viral proteins that may interact with Oas1b, recombinant MBP-Oas1b fusion protein will be used in *in vitro* pull-down and co-immunoprecipitation assays with extracts from C3H.PRI.*Flv'* (resistant) or C3H/He (susceptible) cells. Recombinant MBP-Oas1b protein will also be used for *in vivo* studies of interacting partners using the Chariot protein delivery system (Active Motif).

BIBLIOGRAPHY

- Alexopoulou L, Holt AC, Medzhitov R, Flavell RA. 2001. Recognition of double-stranded RNA and activation of NF-kappaB by Toll-like receptor 3. *Nature*. **413**:732–738.
- Amberg SM, Nestorowicz A, McCourt DW, Rice CM. 1994. NS2B-3 proteinase-mediated processing in the yellow fever virus structural region: In vitro and in vivo studies. *J. Virol.* **68**:3794-3802.
- Au WC, Moore PA, LaFleur DW, Tombal B, Pitha PM. 1998. Characterization of the interferon regulatory factor-7 and its potential role in the transcription activation of interferon A genes. *J. Biol. Chem.* **273**:29210-17.
- Baltimore D. 1968. Structure of the poliovirus replicative intermediate RNA. *J. Mol. Biol.* **32**:359-68.
- Bandyopadhyay SK, Leonard GT, Bandyopadhyay T, Stark GR, Sen GC. 1995. Transcriptional induction by double-stranded RNA is mediated by interferon-stimulated response elements without activation of interferon-stimulated gene factor 3. *J. Biol. Chem* **270**:19624–29.
- Bang FB. 1978. Genetic resistance of animals to viruses: Introduction and studies in mice. *Adv. Virus Res.* **23**:269-348.
- Bauer JH, Mahaffy AF. 1930. Susceptibility of African monkeys to yellow fever. *Am. J. Hyg.* **12**:155-74.
- Bernard KA, Maffei JG, Jones SA, Kauffman EB, Ebel GD, et al. 2001. West Nile virus infection in birds and mosquitoes. *Emerg. Infect. Dis.* **7**, 679-685.
- Bhatt PN, Jacoby RO. 1976. Genetic resistance to lethal flavivirus encephalitis. II. Effect of immunosuppression. *J. Infect. Dis.* **134**:166-173.
- Biron C, Sen GC. 2001. Interferons and other cytokines, pp. 321–351. In D. M. Knipe and P. M. Howley (ed.), *Fields virology*, 4th ed. Lippincott/The Williams & Wilkins Co., Philadelphia, PA.
- Blackwell JL, Brinton MA. 1995. BHK cell proteins that bind to the 3' stem-loop structure of the West Nile virus genome RNA. *J. Virol.* **69**:5650–58.
- Blackwell JL, Brinton MA. 1997. Translation elongation factor-1 α interacts with the 3' stem-loop of West Nile virus genomic RNA. *J. Virol.* **71**:6433–44.

- Bowes C, Li T, Danciger M, Baxter LC, Applebury ML, et al. 1990. Retinal degeneration in the rd mouse is caused by a defect in the beta subunit of rod cGMP-phosphodiesterase. *Nature*. **347**:677-80.
- Brinton Darnell M, Koprowski H. 1974. Genetically determined resistance to infection with group B arboviruses. II. Increased production of interfering particles in cell cultures from resistant mice. *J. Infect. Dis.* **129**: 248-56.
- Brinton Darnell M, Koprowski H, Lagerspetz K. 1974. Genetically determined resistance to infection with group B arboviruses. I. Distribution of the resistance gene among various mouse populations and characteristics of gene expression in vivo. *J. Infect. Dis.* **129**:240-47.
- Brinton MA. 1981. Isolation of a replication-efficient mutant of West Nile virus from a persistently infected genetically resistant mouse cell culture. *J Virol.* **39**:413-21.
- Brinton MA. 1986. *Replication of flaviviruses*. In *Togaviridae and Flaviviridae, The Viruses*, ed. S Schlesinger, M Schlesinger, pp. 329–76. New York: Plenum.
- Brinton MA. 2002. The molecular biology of West Nile Virus: a new invader of the western hemisphere. *Annu. Rev. Microbiol.* **56**:371-402.
- Brinton MA, Arnheiter H, Haller O. 1982. Interferon independence of genetically controlled resistance to flaviviruses. *Infect. Immun.* **36**: 284-88.
- Brinton MA, Dispoto JH. 1988. Sequence and secondary structure analysis of the 5' terminal region of flavivirus genome RNA. *Virology.* **61**:3641-44.
- Brinton MA, Pereygin AA. 2003. Genetic resistance to flaviviruses. *Adv Virus Res.* **60**:43-85.
- Bunning ML, Bowen RA, Cropp CB, Sullivan KG, Davis BS, et al. 2002. Experimental infection of horses with West Nile virus. *Emerg. Infect. Dis.* **8**:380-386.
- Cahour A, Pletnev A, Vazeille-Falcoz M, Rosen L, Lai CJ. 1995. Growth-restricted dengue virus mutants containing deletions in the 5' noncoding region of the RNA genome. *Virology* **207**:68–76.
- Casals J, Schneider HA. 1943. Natural resistance and susceptibility to Russian spring-summer encephalitis in mice. *Proc. Soc. Expl. Biol. Med.* **54**:201-202.
- Centers for Disease Control and Prevention (CDC), DVVID website. 2003. <http://www.cdc.gov/ncidod/dvbid/westnile/background.htm>
- Chambers TJ, Grakoui A, Rice CM. 1991. Processing of the yellow fever virus nonstructural polyprotein: a catalytically active NS3 proteinase domain and NS2B

- are required for cleavages at dibasic sites. *J. Virol.* **65**:6042-50.
- Chambers TJ, Nestorowicz A, Amberg SM, Rice CM. 1993. Mutagenesis of the yellow fever virus NS2B protein: effects on proteolytic processing, NS2B-NS3 complex formation, and viral replication. *J. Virol.* **67**:6797-807.
- Chambers TJ, Nestorowicz A, Rice CM. 1995. Mutagenesis of the yellow fever virus NS2B/3 cleavage site: determinants of cleavage site specificity and effects on polyprotein processing and viral replication. *J. Virol.* **69**:1600-5.
- Chambers TJ, Weir RC, Grakoui A, McCourt DW, Bazan JF, et al. 1990. Evidence that the N-terminal domain of nonstructural protein NS3 from yellow fever virus is a serine protease responsible for site-specific cleavages in the viral polyprotein. *Proc. Natl. Acad. Sci. USA* **87**:8898-902.
- Chang YE, Laimins LA. 2000. Microarray analysis identifies interferon-inducible genes and Stat-1 as major transcriptional targets of human papillomavirus type 31. *J. Virol.* **74**:4174-82.
- Chu PW, Westaway EG. 1985. Replication strategy of Kunjin virus: Evidence for recycling role of replicative form RNA as template in semiconservative and asymmetric replication. *Virology.* **140**:68-79.
- Cleaves GR, Dubin DT. 1979. Methylation status of intracellular dengue type 2 40 S RNA. *Virology.* **96**:159-65.
- Cleaves GR, Ryan TE, Schlesinger RW. 1981. Identification and characterization of type 2 dengue virus replicative intermediate and replicative form RNAs. *Virology.* **111**:73-83.
- Clemens MJ, Elia A. 1997. The double-stranded RNA-dependent protein kinase PKR: structure and function. *J. Interferon Cytokine Res.* **17**:503-24.
- Clemens MJ, Williams BR. 1978. Inhibition of cell-free protein synthesis by pppA2'p5'A2'p5'A: a novel oligonucleotide synthesized by interferon-treated L cell extracts. *Cell.* **13**:565-72.
- Daly C, Reich NC. 1993. Double-stranded RNA activates novel factors that bind to the interferon-stimulated response element. *Mol. Cell Biol.* **13**:3756-64.
- Daly C, Reich NC. 1995. Characterization of specific DNA-binding factors activated by double-stranded RNA as positive regulators of interferon alpha/beta-stimulated genes. *J. Biol. Chem.* **270**:23739-46.
- Darnell JE Jr, Kerr IM, Stark GR. 1994. Jak-STAT pathways and transcriptional activation in response to IFNs and other extracellular signaling proteins. *Science.* **264**:1415-21.

- Der SD, Zhou A, Williams BR, Silverman RH. 1998. Identification of genes differentially regulated by interferon alpha, beta, or gamma using oligonucleotide arrays. *Proc. Natl. Acad. Sci. USA* **95**:15623–28.
- Desai SY, Patel RC, Sen GC, Malhotra P, Ghadge GD, et al. 1995. Activation of interferon-inducible 2'-5' oligoadenylate synthetase by adenoviral VAI RNA. *J. Biol. Chem.* **270**:3454-61.
- Desai SY, Sen GC. 1997. Effects of varying lengths of double-stranded RNA on binding and activation of 2'-5'-oligoadenylate synthetase. *J. Interferon Cytokine Res.* **17**:531-6.
- Durand B, Chevalier V, Pouillot R, Labie J, Marendat I, et al. 2002. West Nile virus outbreak in horses, southern France, 2000: results of a serosurvey. *Emerg. Infect Dis.* **8**:777-782.
- Eskildsen S, Justesen J, Schierup MH, Hartmann R. 2003. Characterization of the 2'-5'-oligoadenylate synthetase ubiquitin-like family. *Nuc. Acids Res.* **31**:3166-73.
- Falgout B, Markoff L. 1995. Evidence that flavivirus NS1-NS2A cleavage is mediated by membrane-bound host protease in the endoplasmic reticulum. *J. Virol.* **69**:7232-43.
- Finter NB. 1996. The naming of cats--and alpha-interferons. *Lancet.* **348**:348-9.
- Geiss GK, Carter VS, He Y, Kwieciszewski BK, Holzman T, et al. 2003. Gene expression profiling of the cellular transcriptional network regulated by alpha/beta interferon and its partial attenuation by the hepatitis C virus nonstructural 5A protein. *J. Virol.* **77**:6367–75.
- Geiss GK, Gin G, Guo J, Bumgarner R, Katze MG, et al. 2001. A comprehensive view of regulation of gene expression by double-stranded RNA-mediated cell signaling. *J. Biol. Chem.* **276**:30178–82.
- Geiss GK, Salvatore M, Tumpey TM, Carter VS, Wang X, et al. 2002. Cellular transcriptional profiling in influenza A virus-infected lung epithelial cells: the role of the nonstructural NS1 protein in the evasion of the host innate defense and its potential contribution to pandemic influenza. *Proc. Natl. Acad. Sci. USA* **99**:10736–41.
- Ghosh A, Sarkar SN, Guo W, Bandyopadhyay S, Sen GC. 1997. Enzymatic activity of 2'-5'-oligoadenylate synthetase is impaired by specific mutations that affect oligomerization of the protein. *J. Biol. Chem.* **272**:33220-26.

- Ghosh A, Sarkar SN, Rowe TM, Sen GC. 2001. A specific isozyme of 2'-5' oligoadenylate synthetase is a dual function proapoptotic protein of the Bcl-2 family. *J Biol. Chem.* **276**:25447-55.
- Goodman GT, Koprowski H. 1962. Study of the mechanism of innate resistance to virus infection. *J. Cell. Comp. Physiol.* **59**: 333-73.
- Groschel D, Koprowski H. 1965. Development of a virus-resistant inbred mouse strain for the study of innate resistance to arbo B viruses. *Arch. Gesamte. Virusforsch.* **18**:379-91.
- Groves MG, Rosenstreich DL, Taylor BA, Osterman JV. 1980. Host defenses in experimental scrub typhus: mapping the gene that controls natural resistance in mice. *J. Immunol.* **125**:1398-99.
- Guo JT, Hayashi J, Seeger C. 2005. West Nile virus inhibits the signal transduction pathway of alpha interferon. *J. Virol.* **79**:1343-50.
- Guzman MG, Kouri GP, Bravo J, Soler M, Vazquez S, et al. 1990. Dengue hemorrhagic fever in Cuba, 1981: a retrospective seroepidemiologic study. *Am. J. Trop. Med. Hyg.* **42**:179-184.
- Han JQ, Barton DJ. 2002. Activation and evasion of the antiviral 2'-5' oligoadenylate synthetase/ribonuclease L pathway by hepatitis C virus mRNA. *RNA* **8**:512-25.
- Hanson B, Koprowski H, Baron S, Buckler CE. 1969. Interferon-mediated natural resistance of mice to arbo B virus infection. *Microbios* **1B**:51-68.
- Hartmann R, Olsen HS, Widder S, Jorgensen R, Justesen J. 1998. p59OASL, a 2'-5' oligoadenylate synthetase like protein: a novel human gene related to the 2'-5' oligoadenylate synthetase family. *Nucleic Acids Res.* **26**:4121-28.
- Hartmann R, Justesen J, Sarkar SN, Sen GC, Yee VC. 2003. Crystal structure of the 2'-specific and double-stranded RNA-activated interferon-induced antiviral protein 2'-5' oligoadenylate synthetase. *Mol. Cell.* **12**:1173-85.
- Heinz FX, Allison SL. 2000. Structures and mechanisms in flavivirus fusion. *Adv. Virus Res.* **55**:231-69.
- Heinz FX, Auer G, Stiasny K, Holzmann H, Mandl C, et al. 1994. The interactions of the flavivirus envelope proteins: implications for virus entry and release. *Arch. Virol. Suppl.* **9**:339-48.

- Heinz FX, Purcell MS, Gould EA, Howard CR, Houghton M, et al. 2000. Family Flaviviridae. In *Virus Taxonomy*, ed. MHV Regenmortel, CM Fauquet, DHL Bishop, EB Carstens, MK Estes, et al., pp. 860-78. San Diego: Academic Press.
- Hori H, Lai CJ. 1990. Cleavage of dengue virus NS1-NS2A requires an octapeptide sequence at the C terminus of NS1. *J. Virol.* **64**:4573-7.
- Hovanessian AG. 1991. Interferon-induced and double-stranded RNA-activated enzymes: a specific protein kinase and 2',5'-oligoadenylate synthetases. *J. Interferon Res.* **11**:199-205.
- Hovanessian AG, Wood JN. 1980. Anticellular and antiviral effects of pppA(2'p5'A)n. *Virology.* **101**:81-90.
- Jerrells TR, Osterman JV. 1981. Host defenses in experimental scrub typhus: inflammatory response of congenic C3H mice differing at the *Ric* gene. *Infect. Immun.* **31**:1014-22.
- Jiang Z, Mak TW, Sen G, Li X. 2004. Toll-like receptor 3-mediated activation of NF-kappaB and IRF3 diverges at Toll-IL-1 receptor domain-containing adapter inducing IFN-beta. *Proc. Natl. Acad. Sci. U S A* **101**:3533-38.
- Johnston C, Jiang W, Chu T, Levine B. 2001. Identification of genes involved in the host response to neurovirulent alphavirus infection. *J. Virol.* **75**:10431-45.
- Juang Y, Lowther W, Kellum M, Au WC, Lin R, et al. 1998. Primary activation of interferon A and interferon B gene transcription by interferon regulatory factor 3. *Proc. Natl. Acad. Sci. USA* **95**:9837-42.
- Kakuta S, Shibata S, Iwakura Y. 2002. Genomic structure of the mouse 2',5'-oligoadenylate synthetase gene family. *J. Interferon Cytokine Res.* **22**:981-993.
- Khromykh AA, Westaway EG. 1996. RNA binding properties of core protein of the flavivirus Kunjin. *Arch. Virol.* **141**:685-99.
- Knipe DM, Howley PM, eds. 2001. *Fields Virology*. Philadelphia: Lippincott, Williams & Wilkins. 4th ed.
- Koonin EV. 1993. Computer-assisted identification of a putative methyltransferase domain in NS5 protein of flaviviruses and lambda 2 protein of reovirus. *J. Gen. Virol.* **74**:733-40.
- Kouri GP, Guzman MG, Bravo JR. 1987. Why dengue haemorrhagic fever in Cuba? 2. An integral analysis. *Trans. R. Soc. Trop. Med. Hyg.* **81**:821-3.

- Kouri GP, Guzman MG, Bravo JR, Triana C. 1989. Dengue haemorrhagic fever/dengue shock syndrome: lessons from the Cuban epidemic, 1981. *Bull. World Health Organ.* **67**: 375-380.
- Kumar A, Yang YL, Flati V, Der S, Kadereit S, et al. 1997. Deficient cytokine signaling in mouse embryo fibroblasts with a targeted deletion in the PKR gene: role of IRF-1 and NF-kappaB. *EMBO J.* **16**:406-16.
- Kuo MD, Chin C, Hsu SL, Shiao JY, Wang TM, et al. 1999. Characterization of the NTPase activity of Japanese encephalitis virus NS3 protein. *J. Gen. Virol.* **77**:2077-84.
- LaVail MM, Sideman RL. 1974. C57BL/6 mice with inherited retinal degeneration. *Arch. Ophthalmol.* **91**:394-400.
- Lengyel P. 1987. Double-stranded RNA and interferon action. *J. Interferon Res.* **7**:511-19.
- Li H, Clum S, You S, Ebner KE, Padmanabhan R. 1999. The serine protease and RNA-stimulated nucleoside triphosphatase and RNA helicase functional domains of dengue virus type 2 NS3 converge within a region of 20 amino acids. *J. Virol.* **73**:3108-16.
- Li, W., Li, Y., Kedersha, N., Swiderick, K, Moreno, T., Anderson, P., and Brinton, M. A. 2002. Cell Proteins, TIA-1 and TIAR, Interact with the 3' Stem Loop of the West Nile virus Complementary Minus Strand RNA. *J. Virol.* **76**: 11989-12000.
- Lin R, Heylbroeck C, Pitha PM, Hiscott J. 1998. Virus-dependent phosphorylation of the IRF-3 transcription factor regulates nuclear translocation, transactivation potential, and proteasome-mediated degradation. *Mol. Cell. Biol.* **18**:2986-96.
- Lin, R.-J., Liao, C.-L., Lin, E., and Lin, Y.-L. 2004. Blocking of the alpha interferon-induced Jak-Stat signaling pathway by Japanese encephalitis virus infection. *J. Virol.* **78**: 9285-94.
- Lindenbach BD, Rice CM. 2001. *Flaviviridae: the viruses and their replication*, p. 991-1041. In D. M. Knipe and P. M. Howley (ed.), *Fields virology*, 4th ed. Lippincott/The Williams & Wilkins Co., Philadelphia, PA.
- Lindenbach BD, Rice CM. 2003. Molecular biology of flaviviruses. *Adv. Virus Res.* **59**:23-61.
- Liu WJ, Chen HB, Wang XJ, Huang H, Khromykh AA. 2004. Analysis of adaptive mutations in Kunjin virus replicon RNA reveals a novel role for the flavivirus nonstructural protein NS2A in inhibition of beta interferon promoter-driven transcription. *J. Virol.* **78**:12225-35.

- Liu WJ, Wang XJ, Mokhonov VV, Shi PY, Randall R, et al. 2005. Inhibition of interferon signaling by the New York 99 strain and Kunjin subtype of West Nile virus involves blockage of STAT1 and STAT2 activation by nonstructural proteins. *J. Virol.* **79**:1934-42.
- Lobigs M. 1993. Flavivirus premembrane protein cleavage and spike heterodimer secretion requires the function of the viral proteinase NS3. *Proc. Natl. Acad. Sci. USA* **90**:6218-22.
- Lyon MF, Kirby MC. 1993. Mouse chromosome atlas. *Mouse Genome.* **91**:40-80.
- Mackenzie JM, Jones MK, Westaway EG. 1999. Markers for trans-Golgi membranes and the intermediate compartment localize to induced membranes with distinct replication functions in flavivirus-infected cells. *J. Virol.* **73**:9555-67.
- Maitra RK, Silverman RH. 1998. Regulation of human immunodeficiency virus replication by 2',5'-oligoadenylate-dependent RNase L. *J. Virol.* **72**:1146-52.
- Marie I, Durbin JE, Levy DE. 1998. Differential viral induction of distinct interferon- α genes by positive feedback through interferon regulatory factor-7. *EMBO J.* **17**:6660-69.
- Mason PW. 1989. Maturation of Japanese encephalitis virus glycoproteins produced by infected mammalian and mosquito cells. *Virology.* **169**:354-64.
- Mathews DH, Sabina J, Zuker M, Turner DH. 1999. Expanded Sequence Dependence of Thermodynamic Parameters Improves Prediction of RNA Secondary Structure. *J. Mol. Biol.* **288**:911-40.
- McAveney KM, Book ML, Ling P, Chebath J, Yu-Lee LY. 2000. Association of 2'-5' oligoadenylate synthetase with the prolactin (PRL) receptor: Alteration in PRL-inducible STA1(signal transducer and activator of transcription 1) signaling to the IRF-1 (interferon-regulatory factor 1) promoter. *Mol. Endocrinology* **14**:295-306.
- Minks MA, West DK, Benveniste S, Baglioni C. 1979. Structural requirements of double-stranded RNA for the activation of 2',5'-oligo(A) polymerase and protein kinase of interferon-treated HeLa cells. *J. Biol. Chem.* **254**:10180-3.
- Mossman KL, Macgregor PF, Rozmus JJ, Goryachev, AB, Edwards AM, et al. 2001. Herpes simplex virus triggers and then disarms a host antiviral response. *J. Virol.* **75**:750-58.
- Munoz-Jordan JL, Laurent-Rolle M, Ashour J, Martinez-Sobrido L, Ashok M, et al. 2005. Inhibition of alpha/beta interferon signaling by the NS4B protein of flaviviruses. *J. Virol.* **79**:8004-13.

- Munoz-Jordan, J.L., Sanchez-Burgos, G.G., Laurent-Rolle, M., and Garcia-Sastre, A. 2003. Inhibition of interferon signalling by dengue virus. *Proc. Natl. Acad. Sci. USA* **100**:14333-38.
- Murphy FA. 1980. *Togavirus morphology and morphogenesis*. In *The Togaviruses: Biology, Structure, Replication*, ed. RW Schlesinger, pp. 241-316. Academic Press, New York.
- Nakaya T, Sato M, Hata N, Asagiri M, Suemori H, et al. 2001. Gene induction pathways mediated by distinct IRFs during viral infection. *Biochem. Biophys. Res. Commun.* **283**:1150-56.
- Nanduri S, Rahman F, Williams BR, Qin J. 2000. A dynamically tuned double-stranded RNA binding mechanism for the activation of antiviral kinase PKR. *EMBO J.* **19**:5567-74.
- Perelygin AA, Lear TL, Zharkikh, Brinton MA. 2004. Structure of equine 2'-5' oligoadenylate synthetase (Oas) gene family and FISH mapping of Oas genes to ECA8p15-p14 and BTA17q24-25. *Cytogenetic and Genome Research*, In Press.
- Perelygin AA, Scherbik SS, Zhulin IB, Stockman BM, Li Y, et al. 2002. Positional cloning of the murine flavivirus resistance gene. *Proc Natl Acad Sci USA* **99**:9322-27.
- Petersen LR, Roehrig JT. 2001. West Nile Virus: a reemerging global pathogen. *Emerg. Infect. Dis.* **7**, 611-614.
- Pethel M, Falgout B, Lai CJ. 1992. Mutational analysis of the octapeptide sequence motif at the NS1-NS2A cleavage junction of dengue type 4 virus. *J. Virol.* **66**:7225-31.
- Poidinger M, Hall RA, Mackenzie JS. 1996. Molecular characterization of the Japanese encephalitis serocomplex of the flavivirus genus. *Virology.* **218**, 417-421.
- Porterfield, JS. 1996. *Encephalitis viruses: encephalitis viruses and related viruses causing hemorrhagic disease*, Academic Press, San Diego, CA.
- Rice CM. 1996. *Flaviviridae: the viruses and their replication*. In *Fields Virology*, ed. BN Fields, DM Knipe, PM Howley, pp. 931-59. Philadelphia: Lippincott-Raven. 3rd ed.
- Rice CM, Lenches EM, Eddy SR, Shin SJ, Sheets RL, et al. 1985. Nucleotide sequence of yellow fever virus: implications for flavivirus gene expression and evolution. *Science* **229**:726-35

- Reid HW, Moss R, Pow I, Buxton D. 1980. The response of three grouse species (*Tetrao urogallus*, *Lagopus mutus*, *Lagopus lagopus*) to louping-ill virus. *J. Comp. Pathol.* **90**:257-63.
- Ruiz MO, Tedesco C, McTighe TJ, Austin C, Kitron U. 2004. Environmental and social determinants of human risk during a West Nile virus outbreak in the greater Chicago area, 2002. *Int. J. Health Geogr.* **3**:8.
- Sabin AB. 1952. Nature of inherited resistance to viruses affecting the nervous system. *Proc. Natl. Acad. Sci. USA* **38**:540-46.
- Samuel CE. 2001. Antiviral actions of interferons. *Clin. Microbiol. Rev.* **14**: 778-809.
- Sangster MY, Heliamas DB, Mackenzie JS, Shellam GR. 1993. Genetic studies of flavivirus resistance in inbred strains derived from wild mice: evidence for a new resistance allele at the flavivirus locus (*Flv*). *J. Virol.* **67**:340-47.
- Sangster MY, Mackenzie JS, Shellam GR. 1998. Genetically determined resistance to flavivirus infection in wild *Mus musculus domesticus* and other taxonomic groups in the genus *Mus*. *Arch. Virol.* **143**:697-715.
- Sangster MY, Urosevic N, Mansfield JP, Mackenzie JS, Shellam GR. 1994. Mapping the *Flv* locus controlling resistance to flaviviruses on mouse chromosome 5. *J. Virol.* **68**:448-52.
- Sarkar SN, Bandyopadhyay S, Ghosh A, Sen GC. 1999. Enzymatic characteristics of recombinant medium isozyme of 2'-5' oligoadenylate synthetase. *J. Biol. Chem.* **274**:1848-55.
- Sarkar SN, Miyagi M, Crabb JW, Sen GC. 2002. Identification of the substrate binding sites of 2'-5' Oligoadenylate synthetase. *J. Biol. Chem.* **277**:4321-30.
- Sarkar SN, Sen GC. 2004. Novel functions of proteins encoded by viral stress-inducible genes. *Pharmacology and Therapeutics.* **103**:245-59.
- Sato M, Hata N, Asagiri M, Nakaya T, Taniguchi T, et al. 1998a. Distinct and essential roles of transcription factors IRF-3 and IRF-7 in response to viruses for IFN- α/β gene induction. *Immunity* **13**:539-548.
- Sato M, Tanaka N, Hata N, Oda E, Taniguchi T. 1998b. Involvement of the IRF family transcription factor IRF-3 in virus-induced activation of the IFN- β gene. *FEBS Lett.* **425**:112-116.
- Sharp TV, Raine DA, Gewert DR, Joshi B, Jagus R, et al. 1999. Activation of the interferon-inducible (2'-5') oligoadenylate synthetase by the Epstein-Barr virus RNA, EBER-1. *Virology.* **257**:303-13.

- Shellam GR, Sangster MY, Urosevic N. 1998. Genetic control of host resistance to flavivirus infection in animals. *Rev. Sci. Tech.* **17**:231-48.
- Shellam GR, Urosevic N, Sangster MY, Mansfield JP, et al. 1993. Characterization of allelic forms at the retinal degeneration (rd) and b-glucuronidase (Gus) loci for the mapping of the flavivirus resistance (Flv) gene on mouse chromosome 5. *Mouse Genome* **91**: 572-74.
- Shi P-Y, Li W, Brinton MA. 1996. Cell proteins bind specifically to West Nile virus minus-strand 3' stem-loop RNA. *J. Virol.* **70**:6278-87.
- Silverman RH, Cirino NM. 1997. *mRNA metabolism and post-translational gene regulation.* pp.295-309. In: D.R. Morris and J.B. Hartford, Editors, *Gene Regulation*, Wiley, New York.
- Smithburn KC, Haddow AJ. 1949. The susceptibility of African wild animals to yellow fever. *Am. J. Trop. Med.* **29**:389-423.
- Smithburn KC, Hughes TP, Burke AW, Paul JH. 1940. A neurotropic virus isolated from the blood of a native of Uganda. *Am. J. Trop. Med. Hyg.* **20**, 471-492.
- Stadler K, Allison SL, Schalich J, Heinz FX. 1997. Proteolytic activation of tick-borne encephalitis virus by furin. *J. Virol.* **71**:8475-81.
- Stark GR, Kerr IM, Williams BR, Silverman RH, Schreiber RD. 1998. How cells respond to interferons. *Annu. Rev. Biochem.* **67**:227-64.
- Urosevic N, Silvia OJ, Sangster MY, Mansfield JP, Hodgetts SI, et al. 1999. Development and characterization of new flavivirus-resistant mouse strains bearing *Flv^r*-like and *Flv^{mr}* alleles from wild or wild-derived mice. *J. Gen. Virol.* **80**:897-906.
- Urosevic N, Mann K, Hodgetts SI, Shellam GR. 1997. The use of microsatellites in high-resolution genetic mapping around the mouse flavivirus resistance locus (*Flv*). *Arbovirus Res. Aust.* **7**:296-99.
- Vianio T. 1963. Virus and hereditary resistance in vitro behavior of West Nile (E101) virus in cultures prepared from genetically resistant and susceptible strains of mice. *Ann. Med. Exp. Biol. Fenn.* **41**:1-24.
- Wathelet MG, Lin CH, Parekh BS, Ronco LV, Howley PM, et al. 1998. Virus infection induces the assembly and coordinately activated transcription factors on the IFN- β enhancer in vivo. *Mol. Cell.* **1**:507-18.

- Weaver BK, Kumar KP, Reich NC. 1998. Interferon regulatory factor 3 and CREB-binding protein/p300 are subunits of double-stranded RNA-activated transcription factor DRAF1. *Mol. Cell. Biol.* **18**:1359-68.
- Webster LT. 1923. Microbic virulence and host susceptibility in mouse typhoid infection. *J. Exp. Med.* **37**:231-44.
- Webster LT. 1933. Inherited and acquired factors in resistance to infection. I. Development of resistant and susceptible lines of mice through selective breeding. *J. Exp. Med.* **57**:793-817.
- Webster LT. 1937. Inheritance of resistance of mice to enteric bacterial and neurotropic virus infections. *J. Exp. Med.* **65**:261-86.
- Webster LT, Johnson MS. 1941. Comparative virulence of St Louis encephalitis virus cultured with brain tissue from innately susceptible and innately resistant mice. *J. Exp. Med.* **74**:489-94.
- Wengler G. 1989. Cell-associated West Nile flavivirus is covered with E+ pre-M protein heterodimers which are destroyed and reorganized by proteolytic cleavage during virus release. *J. Virol.* **63**:2521-26.
- Wengler G, Wengler G. 1991. The carboxy-terminal part of the NS3 protein of the West Nile flavivirus can be isolated as a soluble protein after proteolytic cleavage and represents an RNA-stimulated NTPase. *Virology* **184**:707-15.
- Wengler G, Wengler G, Gross HJ. 1978. Studies on virus-specific nucleic acids synthesized in vertebrate and mosquito cells infected with flaviviruses. *Virology.* **89**:423-37.
- Wreschner DH, McCaule JW, Skehel JJ, Kerr IM. 1981. Interferon action--sequence specificity of the ppp(A2'p)nA-dependent ribonuclease. *Nature* **289**:414-17.
- Yamshchikov VF, Compans RW. 1994. Processing of the intracellular form of the west Nile virus capsid protein by the viral NS2B-NS3 protease: an in vitro study. *J. Virol.* **68**:5765-71.
- Yan W, Lang M, Stein P, Pangas SA, Burns KH, et al. 2005. Mice deficient in oocyte-specific oligoadenylate synthetase-like protein OAS1D display reduced fertility. *Mol. Cell. Biol.* **25**:4615-24.
- Yoneyama M, Suhara W, Fukuhara Y, Fukuda M, Nishida, E, et al. 1998. Direct triggering of the type I interferon system by virus infection: activation of a transcription factor complex containing IRF-3 and CBP/p300. *EMBO J.* **17**:1087-95.
- You S, Falgout B, Markoff L, Padmanabhan R. 2001. In vitro RNA synthesis from

exogenous dengue viral RNA templates requires long-range interactions between 5'- and 3'-terminal regions that influence RNA structure. *J. Biol. Chem.* **276**:15581-91.

Zhou A, Hassel BA, Silverman RH. 1993. Expression cloning of 2-5A-dependent RNAase: a uniquely regulated mediator of interferon action. *Cell.* **72**:753-65.

Zhu H, Cong JP, Mamtora G, Gengiras T, Shenk T. 1998. Cellular gene expression altered by human cytomegalovirus: global monitoring with oligonucleotide arrays. *Proc Natl Acad Sci USA* **95**:14470-75.

Zucher M. 2003. Mfold web server for nucleic acid folding and hybridization prediction. *Nucleic Acids Res.* **31**:3406-15.